iScience

CellPress

Article

Chromosome-Level Genome Reveals the Origin of Neo-Y Chromosome in the Male Barred Knifejaw *Oplegnathus fasciatus*

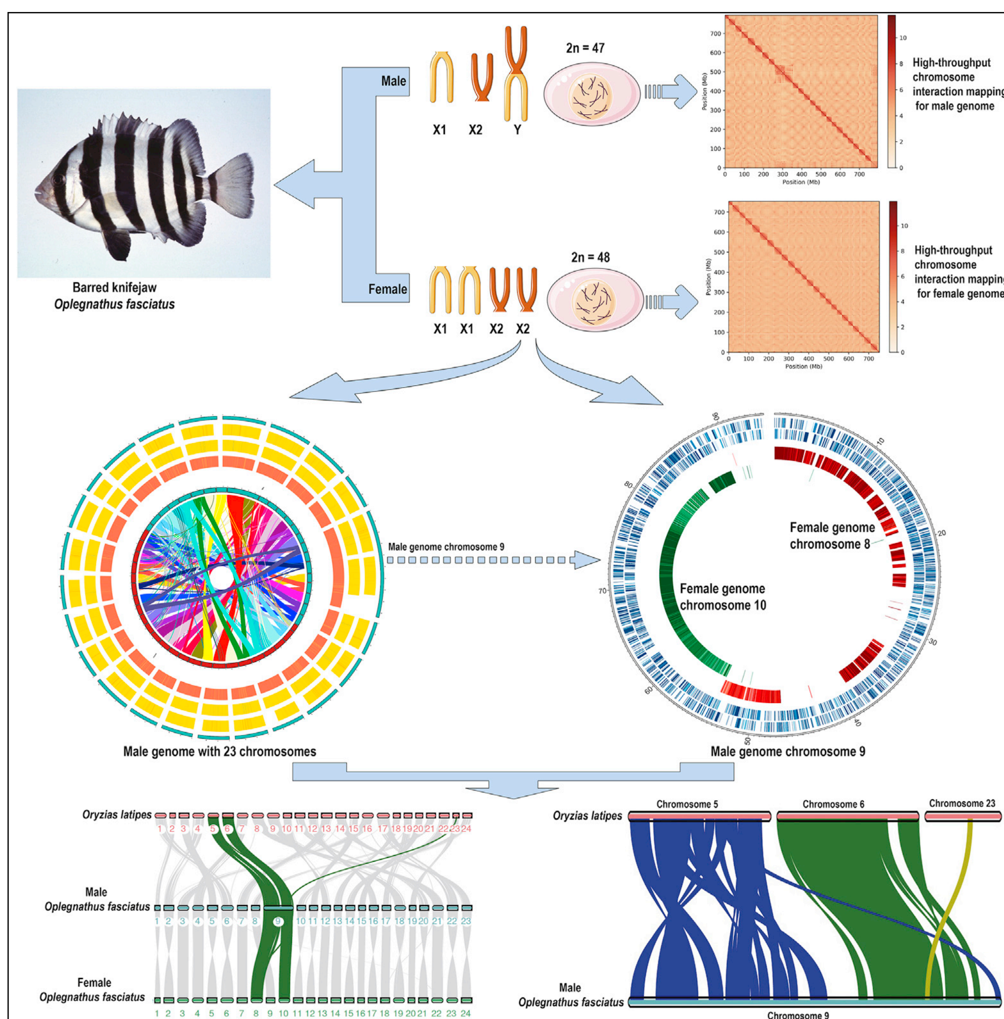

Yongshuang Xiao, Zhizhong Xiao, Daoyuan Ma, ..., Jing Liu, Jun Li, Angel Herrera-Ulloa

shijun_xiao@163.com (S.X.)
jliu@qdio.ac.cn (J.L.)
junli@qdio.ac.cn (J.L.)

HIGHLIGHTS

Construction of a chromosome-level reference genome for the male *O. fasciatus*

Identification of the origin of neo-Y chromosome to the X_1X_2Y system

Accurate comparisons of sequences and genes between female $X_1X_1X_2X_2$ and male X_1X_2Y

Xiao et al., iScience *23*, 101039
April 24, 2020 © 2020 The Author(s).
https://doi.org/10.1016/j.isci.2020.101039

iScience

CellPress

Article

Chromosome-Level Genome Reveals the Origin of Neo-Y Chromosome in the Male Barred Knifejaw *Oplegnathus fasciatus*

Yongshuang Xiao,[1,2,8] Zhizhong Xiao,[1,2,8] Daoyuan Ma,[1,2] Chenxi Zhao,[3] Lin Liu,[4] Hao Wu,[4] Wenchao Nie,[4] Shijun Xiao,[5,6,*] Jing Liu,[1,2,*] Jun Li,[1,2,9,*] and Angel Herrera-Ulloa[7]

SUMMARY

The barred knifejaw, *Oplegnathus fasciatus*, is characterized by an X_1X_2Y system with a neo-Y chromosome for males. Here, a chromosome-level genome was assembled to investigate the origin of neo-Y chromosome to the male *O. fasciatus*. Twenty-three chromosomes corresponding to the male karyotypes were scaffolded to 762-Mb genome with a contig N50 length of 2.18 Mb. A large neo-Y chromosome (*Ch9*) in the male *O. fasciatus* genome was also assembled and exhibited high identity to those of the female chromosomes *Ch8* and *Ch10*. Chromosome rearrangements events were detected in the neo-chromosome *Ch9*. Our results suggested that a centric fusion of acrocentric chromosomes *Ch8* and *Ch10* should be responsible for the formation of the X_1X_2Y system. The high-quality genome will not only provide a solid foundation for further sex-determining mechanism research in the X_1X_2Y system but also facilitate the artificial breeding aiming to improve the yield and disease resistance for *Oplegnathus*.

INTRODUCTION

The barred knifejaw (*Oplegnathus fasciatus*) (FishBase ID: 1709; NCBI Taxonomy ID: 163134) (Temminck and Schlegel, 1844), a member of the Oplegnathidae family of the Centrarchiformes, is a commercially important rocky reef fish native to East Asia. *O. fasciatus* has become an important fishery resource in offshore cage aquaculture and fish stocking for marine ranching in China, Japan, and Korea (Schembri et al., 2010; Xiao et al., 2016, 2019). This fish is also a valuable species for sashimi and recreational fishing, and its ex-factory price has reached up to $30 per kilogram in China (Xiao, 2015; Park et al., 2018). It has been reported that the male of *O. fasciatus* has 2n = 47 chromosomes (1m + 2m/sm + 44t), whereas the females possess 2n = 48 chromosomes (2m/sm + 46t) (Xu et al., 2012, 2019). Similar chromosome karyotypes have also been reported in male and female individuals of Oplegnathus *punctatus* (Xue et al., 2016; Xu et al., 2019). A large metacentric Y chromosome was found in male individuals of *O. fasciatus* and *O. punctatus* based on karyotypes and microsatellite DNA motif analyses, and it was suggested that the sex-determining types of *O. fasciatus* and *O. punctatus* should belong to the multiple $X_1X_1X_2X_2/X_1X_2Y$ sexual system (Xu et al., 2012, 2019; Xue et al., 2016). Sexual dimorphism in growth has been detected in *O. fasciatus*, with male fish exhibiting faster growth than females, possibly due to the sex chromosome system in *Oplegnathus* (Xiao, 2015). *O. fasciatus* is vulnerable to viruses (e.g., iridovirus) due to inbreeding in aquaculture industry (Li et al., 2011; Zhang et al., 2014). Its high aquaculture value, multiple $X_1X_1X_2X_2/X_1X_2Y$ sex chromosome system, and susceptibility to widespread biotic diseases have led to increasing research interests in *O. fasciatus*. Although the previous reports provided a preliminary description of the multiple sex chromosome system, the exact origin and molecular composition of the large metacentric Y chromosome of the X_1X_2Y system at the genomic level remain unclear.

Approximately 37 cases of multiple sex chromosomes with $X_1X_1X_2X_2/X_1X_2Y$ system have been reported across the teleost phylogeny (Sember et al., 2015; Bitencourt et al., 2016; Zhang et al., 2018; Krysanov and Demidova, 2018; Cai et al., 2019; Xu et al., 2019). A preliminary description of those multiple sex chromosome systems, including karyotypes, C-bands, rDNA locations, karyotype diversification, and identification of sex-specific regions at the cytogenetic level, has been carried out based on conventional cytogenetic (Giemsa-staining and C-banding) and molecular cytogenetic protocols (repetitive DNA markers, comparative genomic hybridization, and whole-chromosome painting) (Parise-Maltempi et al., 2007; Cioffi and Bertollo, 2012; Blanco et al., 2013; Sember et al., 2015; Ferreira et al., 2016; Bitencourt et al., 2016).

[1]Center for Ocean Mega-Science, The Key Laboratory of Experimental Marine Biology, Institute of Oceanology, Chinese Academy of Sciences, Qingdao, China

[2]Laboratory for Marine Biology and Biotechnology, Qingdao National Laboratory for Marine Science and Technology, Qingdao, China

[3]BGI Education Center, University of Chinese Academy of Sciences, Shenzhen, China

[4]Wuhan Frasergen Bioinformatics Co., Ltd. East Lake High-Tech Zone, Wuhan, China

[5]College of Plant Protection, Jilin Agriculture University, Changchun, Jilin, China

[6]School of Computer Science and Technology, Wuhan University of Technology, Wuhan, China

[7]Escuela de Ciencias Biológicas, Universidad Nacional, San José, Costa Rica

[8]These authors contributed equally

[9]Lead Contact

*Correspondence: shijun_xiao@163.com (S.X.), jliu@qdio.ac.cn (J.L.), junli@qdio.ac.cn (J.L.)

https://doi.org/10.1016/j.isci.2020.101039

This is an open access article under the CC BY-NC-ND license (http://creativecommons.org/licenses/by-nc-nd/4.0/).

However, adequate genome resources to support more comprehensive descriptions of the multiple sex chromosome system and the origin of the large metacentric Y chromosome of male *O. fasciatus* have been lacking. The recent release of the chromosome-level reference genome of female *O. fasciatus* has provided valuable resource for sex-determination studies; however, a female genome is still needed to investigate the origin of the unique X_1X_2Y system for male *O. fasciatus* (Xiao et al., 2019). Using PacBio sequencing and high-throughput chromosome interaction mapping (Hi-C), Xiao et al. (2019) obtained a chromosome-level reference genome of the female *O. fasciatus* with a final size of 768.8 Mb and a contig and scaffold N50 length of 2.1 Mb and 33.5 Mb, respectively (Xiao et al., 2019). Twenty-four chromosomes corresponding to the female karyotype (2n = 48) were assembled at the genome level. Although the high-quality genome of female *O. fasciatus* provides a valuable genomic resource for further study of breeding systems, it could not be used to identify the origin of the large metacentric Y chromosome of male *O. fasciatus* without a male genome.

Here, we report the chromosome-level genome assembly of male *O. fasciatus* based on PacBio long-read sequencing and Hi-C. Genomic comparisons between male and female *O. fasciatus* were carried out to provide insights into the origin of the X_1X_2Y system of male *O. fasciatus* based on the chromosome-level genome, which has excellent continuity at the contig and scaffold levels. The genome of male *O. fasciatus* can lay a solid foundation for further study of sex-determining mechanisms of the X_1X_2Y system and will provide valuable genomic data for conservation genetics and resistance breeding of *Oplegnathus*.

RESULTS

PacBio Sequencing and Genome Assembly

Two 20-kb PacBio long-read DNA libraries were constructed using the standard protocol provided by the PacBio Sequel platform. A total of ~39.79 Gb of subreads were obtained using SMRT LINK 5.0 to remove the adaptor sequences from the raw data derived from the zero-mode waveguide (Tables 1 and S1). Approximately 4.71 million sequences with an average length of 8.45 kb were obtained for the draft genome assembly of male *O. fasciatus* (Table 1).

To increase the continuity and completeness of the genome assembly, four processes were carried out for the contig assembly. First, the Canu v1.4 software was used to assemble an initial genome of male *O. fasciatus* (Koren et al., 2017). As a result, a total length of 866.9 Mb, including 4,453 contigs with an N50 length of 1.73 Mb, was obtained (Table S2). Second, Redundans v0.13c software was employed to remove sequence redundancies in the initial assembled genome to obtain a 794.8-Mb genome with a contig N50 length of 2.13 Mb (Table S2). Third, Arrow tool implemented in SMRT Link 5.0 software and Pilon v.122 was applied to perform error correction using long read data and Illumina NGS data mentioned in the genome survey analysis (Table S2) (Walker et al., 2014; Xiao et al., 2019). The final contig assembly of 795.1 Mb with a contig N50 length of 2.13 Mb was obtained. The genome contained 2,295 contigs with a longest contig of 9.8 Mb (Tables S2 and S3). A total of 881 contigs were longer than 100 kb, representing 92.6% of the total 794.8 Mb for the male *O. fasciatus* genome (Table 1). The GC content of the contig assembly genome was 40.87% (Figures S1 and S2).

To obtain the chromosome-level genome of male *O. fasciatus*, the Illumina HiSeq X Ten platform was used to generate ~95.9 Gb clean data from the Hi-C library (Tables S1 and S4). According to the abovementioned mapping strategy, more than 95.5% of total reads mapped to the assembled genome in pairs and ~32.5% of read pairs mapped to different contigs. Lachesis software was used to cluster, order, and orientate contigs along chromosomes based on their interaction frequencies. As a result, 1,355 contigs were successfully anchored and oriented into 23 chromosomes, which was consistent with the previous karyotype analyses of male *O. fasciatus* (X_1X_2Y system) (Table S4 and Figure 1) (Xu et al., 2012). The total length of anchored contigs was ~762.2 Mb, representing 95.9% of all assembled contigs. Finally, we obtained the chromosome assembly with a contig N50 length of 2.18 Mb and a scaffold N50 length of 32.4 Mb (Table 1). Obviously, a large neo-chromosome (*Ch9*) showed strong interaction signals from two genomic blocks, corresponding to the *Ch8* and *Ch10* in female *O. fasciatus* ($X_1X_1X_2X_2$ system) (Figure 1) (Xu et al., 2012). Therefore, *Ch9* was likely to be the large metacentric Y chromosome of male *O. fasciatus*. This chromosome (*Ch9*) was scaffolded from 444 contigs and was 94.2 Mb, more than three times larger than any other chromosome (Figures 1, 2, and 3). More than 99.7% of contigs longer than 100kb were anchored on chromosomes, exhibiting the excellent anchoring rate for male *O. fasciatus* chromosome assembly (Table S4).

	Draft Scaffolds for Male *O. fasciatus*	Chromosome-Length Scaffolds Based on Hi-C for Male *O. fasciatus*	[a]Chromosome-Length Scaffolds Based on Hi-C for Female *O. fasciatus*
Genome assembly			
Length of genome (bp)	795,074,755	762,267,613	768,808,243
Number of contigs	2,295	1,355	1,372
Contigs N50 (bp)	2,127,178	2,183,645	2,130,780
Number of scaffold	/	23	24
Scaffold N50 (bp)	/	32,431,321	33,548,962
Genome coverage (X)	251.1		314.6
Number of contigs (≥100 kb)	881	891	708
Total length of contigs (≥100 kb)	736,155,642	733,715,954	732,827,446
Mapping rate of contigs (≥100 kb) (%)	/	99.67	99.67
Genome annotation			
Protein-coding gene number	24,835		24,003
Mean transcript length (kb)	15.8		16.1
Mean exons per gene	10.0		10.1
Mean exon length (bp)	220.1		217.7
Mean intron length (bp)	1,511.7		1,527.4

Table 1. Summary of Male *O. fasciatus* Genome Assembly and Annotation

[a]The data were cited from the reference (Yongshuang Xiao, Zhizhong Xiao, Daoyuan Ma, Jing Liu, Jun Li. Genome sequence of the barred knifejaw *Oplegnathus fasciatus* (Temminck and Schlegel, 1844): the first chromosome-level draft genome in the family Oplegnathidae, GigaScience, Volume 8, Issue 3, March 2019, giz013, doi.org/10.1093/gigascience/giz013).

Genome Quality Evaluation

The Minimap2 software was employed to evaluate the completeness and homogeneity of the assembled genome of male *O. fasciatus* by using the CLR subreads (Table S5). The mapping rate and the coverage of the assembled genome reached 87.6% and 99.9%, respectively (Table S5). These results showed the high completeness and homogeneity of the genome assembly of male *O. fasciatus*. BUSCO v3.0 software with the actinopterygii_odb9 database was employed to further evaluate the completeness of the assembled genome (Simão et al., 2015). The result showed that 97.2% and 1.0% of the 4,456 conserved single-copy orthologous genes were identified as complete BUSCO and fragmented BUSCO profiles in the genome assembly, respectively (Table 2). Among the 4,456 conserved single-copy orthologous genes, 4,210 (91.8%) and 246 (5.4%) genes were identified as single-copy and duplicated BUSCOs, respectively (Table 2). Approximately 80 single-copy orthologous genes were not detected in the actinopterygii_odb9 database. Then, SNP calling data were used to evaluate the accuracy of the male *O. fasciatus* genome assembly, which was generated from the alignment of next-generation sequencing-based short reads to the assembled genome by using BWA and GATK software. Approximately 1.87 million SNP loci were identified, including 1.86 and 0.01 million heterozygous homologous SNPs, respectively (Table S6). The heterozygous SNPs accounted for 0.23% of the male *O. fasciatus* genome, which was comparable with our previous study of the heterozygosity for the female *O. fasciatus* genome (Table S6) (Xiao et al., 2019).

Repetitive Element Identification and Protein Gene Annotation

Approximately 33.5% of the assembled genome was identified as repetitive elements, including repetitive sequences accounting for 23.16% of the male *O. fasciatus* genome based on the *de novo* repeat library

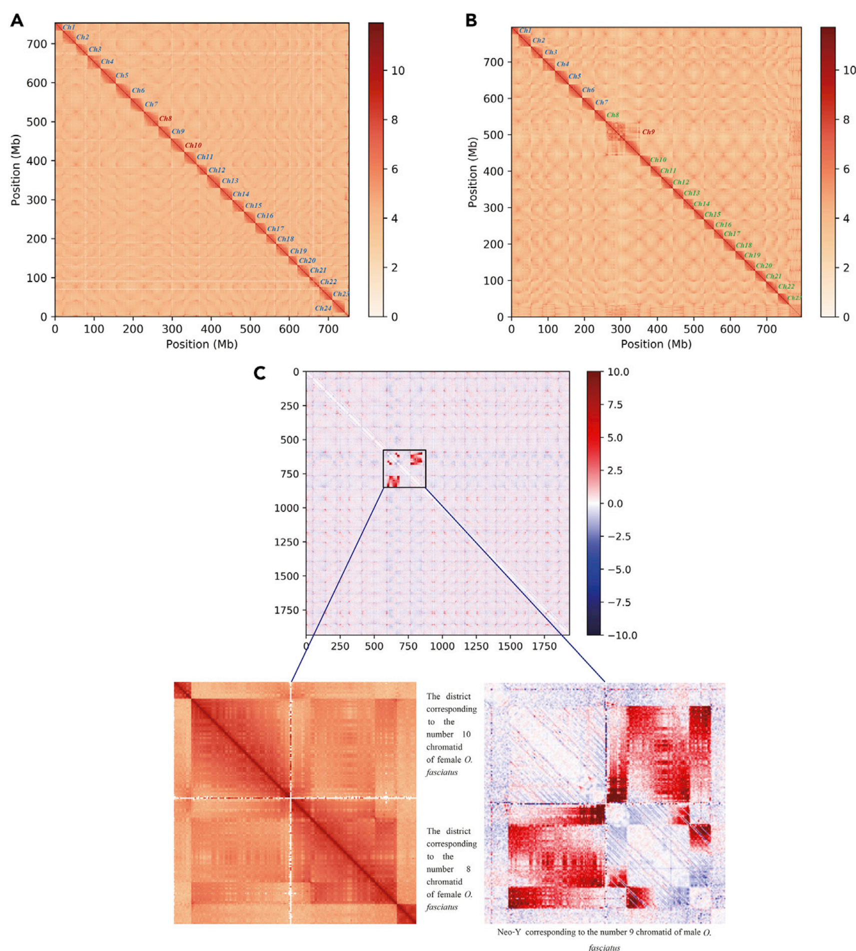

Figure 1. Genome Assembly of Female and Male *O. fasciatus* Based on the Hi-C Interaction Analyses

(A) The heatmap of interactions among genomic bins of 500 kb along 24 chromosomes for female *O. fasciatus* (The data were cited from Xiao et al., 2019).

(B) The heatmap of interactions among genomic bins of 500 kb along 23 chromosomes for male *O. fasciatus*.

(C) The cumulative distribution of subtraction Hi-C Z-scores for interactions between 400- and 40-kb bins from the whole-genome and chromosome levels. Blocks represent the interactions among genomic bins, and the interaction strength was represented by the color scheme from deep (strong interactions) to light (weak interactions). A large neo-chromosome (*Ch9*) was assembled in the male *O. fasciatus* reference genome.

(Table 3). The estimation of repetitive element content for the male *O. fasciatus* genome was comparable to the result of the *k*-mer analysis (38.4%) (Table 3) (Xiao et al., 2019). Interspersed repetitive elements accounting for 22.0% of the male *O. fasciatus* genome were identified, including DNA transposons (10.55%), long interspersed nuclear elements (LINEs, 7.08%), and long terminal repeats (LTRs, 4.11%) (Tables 3 and Table S7 and Figure S3). The repetitive contents of the male *Ch9* and the female *Ch8*/*Ch10* were also identified as 23.79%, 26.07%, and 22.70%, respectively (Table S8). Although the frequency of DNA transposons, LINEs, and LTRs was higher than that in *Larimichthys crocea*, *Gasterosteus aculeatus*, *Oryzias latipes*, and *Dicentrarchus labrax*, the top three categories of TEs were significantly less frequent than in *Epinephelus lanceolatus* and *Triplophysa tibetana* (Table S7).

Homology-based, *de novo,* and transcriptome sequencing-based approaches were integrated to predict protein-coding genes. As a result, 24,835 genes were annotated with an average of 10.0 exons per gene in the male *O. fasciatus* genome (Tables S9 and S10). The distribution statistics of average gene length, average coding sequence (CDS) length, average exons per gene, average exon length, and average intron length of protein-coding genes were also compared with those of six related species (*Lates calcarifer*, *L. crocea*, *G. aculeatus*, *Gadus morhua*, *Panaeolus olivaceus* and *Cynoglossus semilaevis*) and showed a

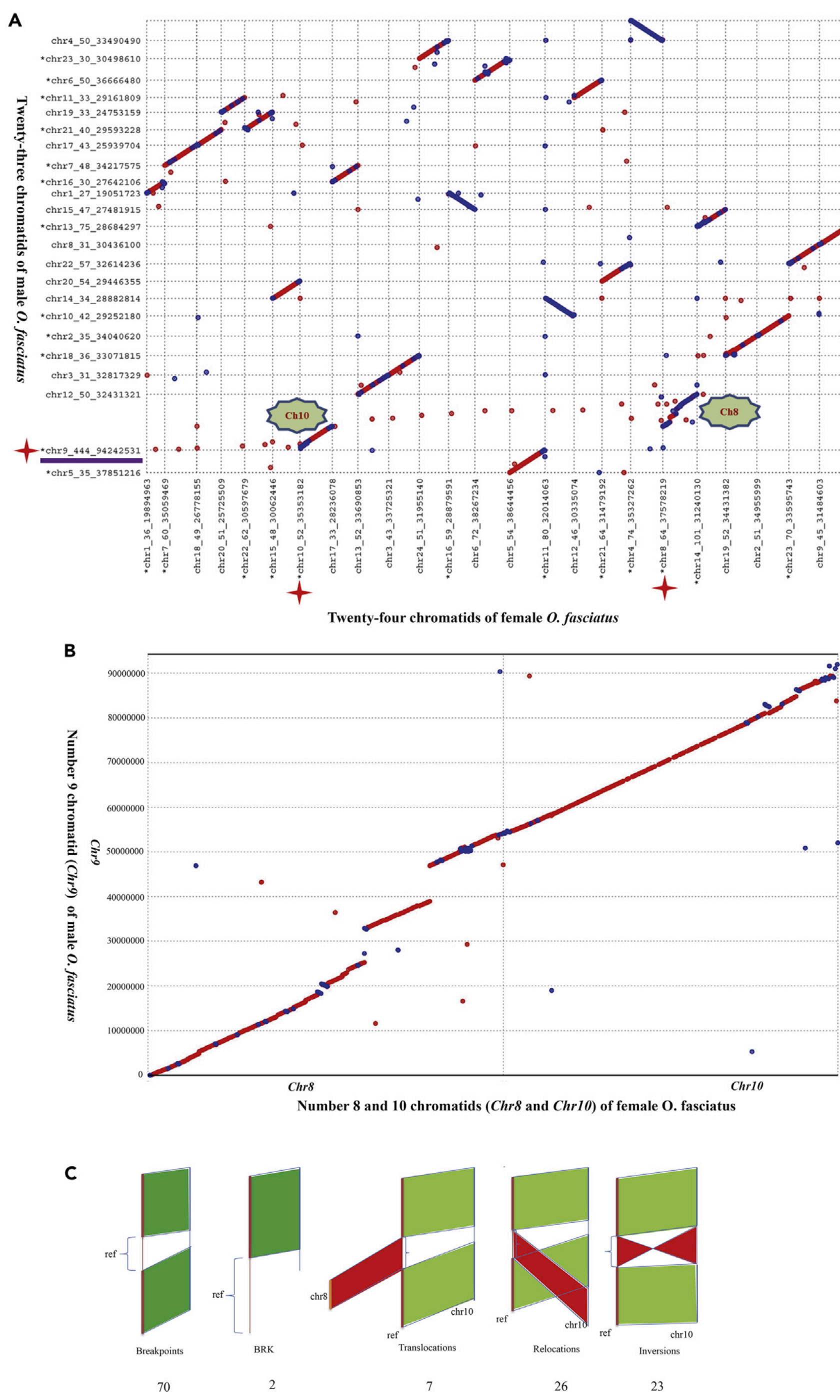

Figure 2. Genomic Comparisons between Female and Male *O. fasciatus*

(A) Genomic comparisons of the whole genome by direct sequence alignment. The majority of female and male *O. fasciatus* chromosomes exhibited 1:1 correspondence except for the large neo-chromosome (*Ch9*).

(B) Detailed genomic comparisons between *Ch9* and *Ch8*/*Ch10* from male and female genomes. The large neo-chromosome (*Ch9*) of the male *O. fasciatus* genome showed largely synteny with the *Ch8* and *Ch10* of the female *O. fasciatus* genome.

(C) The statistics of structure variants with length more than 10 kb between *Ch9* and *Ch8*/*Ch10* from male and female genomes.

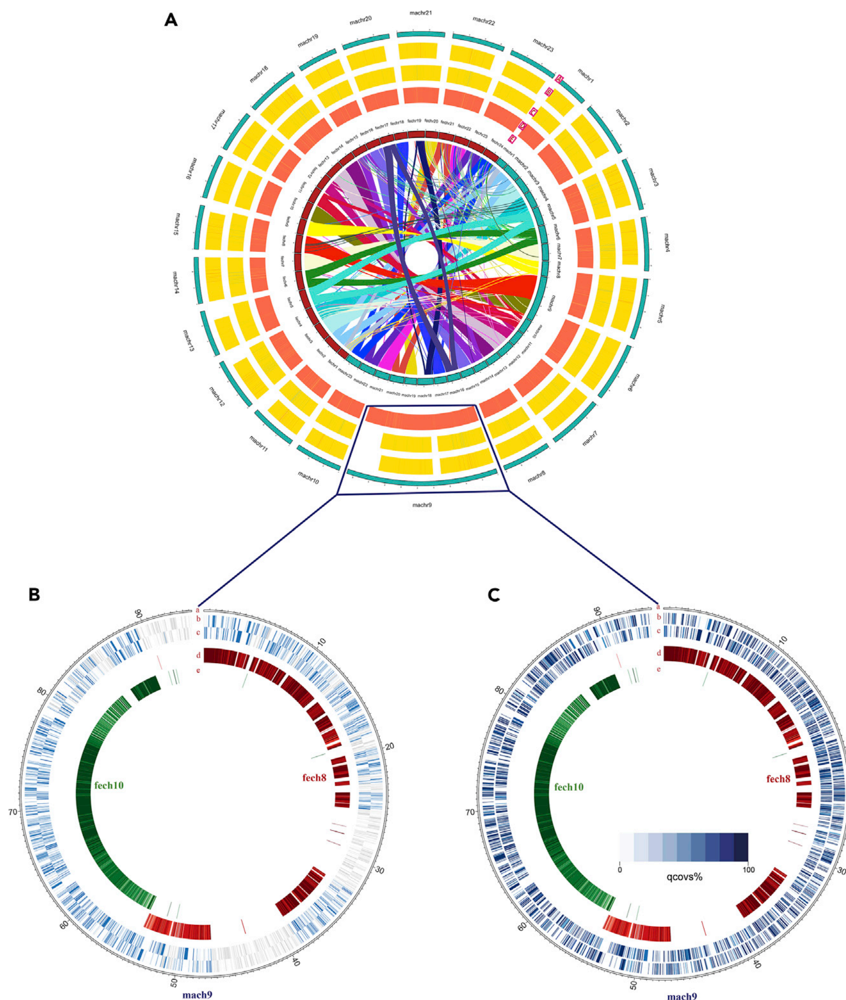

Figure 3. Genome Comparisons Among Male/Female *O. fasciatus* and *L. crocea*

(A) From outer to inner circles: A, 23 chromosomes of male *O. fasciatus*; B, 24 chromosomes of *L. crocea*. The yellow color represents the whole chromosomes and the red lines in the yellow areas represent the common chromosomal region with the male *O. fasciatus*. C, 24 chromosomes of female *O. fasciatus*. The yellow color represents the whole chromosome, and the blue lines in the yellow areas represent the common chromosomal region with the male *O. fasciatus*. D, 23 chromosomes of male *O. fasciatus*. The red color represents the whole chromosome, and the yellow lines in the red areas represent the common chromosomal region with the female *O. fasciatus* and *L. crocea*. E, the red color represents the chromosomes of female *O. fasciatus,* and the green color represents the male *O. fasciatus*. Each line precisely joined pairs of genes originated from the male and female *O. fasciatus* chromosomes.

(B) and (C) From outer to inner circles: a, the ninth chromosome (*Ch9*) of male *O. fasciatus* with coordinate; b, the distribution of forward protein-coding genes in male *Ch9*; c, the distribution of reverse protein-coding genes in male *Ch9*; d, the chromosomal region of male *Ch9* aligned to *Ch8* of female *O. fasciatus* with red color; e, the chromosomal region of male *Ch9* aligned to *Ch10* of female *O. fasciatus* with green color. The gray color represents the distribution of protein-coding genes in unique genomic regions of male *Ch9* (b, c tracks of figure (B)). The color gradient corresponds to the degree of similarities for male *Ch9* genes with the female genes in tracks b and c of figure (C).

similar distribution with those of other teleosts (Figure S4 and Table S10). The average gene length and CDS reached 15,819.4 bp and 1,707.0 bp, respectively (Table S10). Functional annotation of predicted genes in the male *O. fasciatus* genome was further performed using the InterPro, Swiss-Prot, TrEMBL, NR, GO, and KEGG databases (Table 4). Approximately 23,364 of the 24,835 genes (97.34%) in the male *O. fasciatus* genome could be functionally annotated by at least one of the abovementioned databases (Table 4). We used BUSCO v3.0 software to further evaluate the completeness of the annotated genome against actinopterygii_odb9 in the OrthoDB database (Simão et al., 2015). Approximately 96.8% complete BUSCO genes were successfully identified (Table 3). We also used tRNAscan-SE software to annotate the

Type	Assembly		Annotation	
	Proteins	Percentage (%)	Proteins	Percentage (%)
Complete BUSCOs	4,456	97.2	4,435	96.8
Complete and single-copy BUSCOs	4,210	91.8	4,143	90.4
Complete and duplicated BUSCOs	246	5.4	292	6.4
Fragmented BUSCOs	48	1.0	66	1.4
Missing BUSCOs	80	1.8	83	1.8
Total BUSCOs groups searched	4,584	100.0	4,584	100.0

Table 2. Genome Quality of *O. fasciatus* Based on the BUSCO Assessment

non-coding RNAs against the Rfam database, and four types of non-coding RNAs (miRNAs [0.006%], tRNAs [0.009%], rRNAs [0.007%], and small nucleolar RNAs [0.015%]), including 2,666 copies with a total length of 291,392 bp (0.037% of the whole genome) were identified (Table S11).

Chromosome Comparison of Female/Male *O. fasciatus*

According to the synteny-based chromosome comparison between the male and female *O. fasciatus* genomes using the program MUMmer, we found excellent consistency of genome sequences in corresponding chromosomes (Figures 2 and 3). The genome sequences from male *O. fasciatus* had high identity (~99.0%) to those from female *O. fasciatus*, as follows: male *Ch1*/female *Ch1* (99.0%), male *Ch2*/female *Ch2* (99.1%), male *Ch3*/female *Ch3* (99.2%), male *Ch4*/female *Ch4* (99.0%), male *Ch5*/female *Ch5* (99.2%), male *Ch6*/female *Ch6* (99.2%), male *Ch7*/female *Ch7* (99.2%), male *Ch8*/female *Ch9* (99.2%), male *Ch10*/female *Ch11* (99.1%), male *Ch11*/female *Ch12* (99.1%), male *Ch12*/female *Ch13* (99.1%), male *Ch13*/female *Ch14* (99.1%), male *Ch14*/female *Ch15* (99.1%), male *Ch15*/female *Ch16* (99.3%), male *Ch16*/female *Ch17* (99.1%), male *Ch17*/female *Ch18* (99.2%), male *Ch18*/female *Ch19* (99.2%), male *Ch19*/female *Ch20* (99.1%), male *Ch20*/female *Ch21* (99.1%), male *Ch21*/female *Ch22* (99.2%), male *Ch22*/female *Ch23* (99.2%), and male *Ch23*/female *Ch24* (99.2%). The comparisons of chromosomal sequences of female *Ch8*/*Ch10* and the male *Ch9* were further performed (Figure 3B). A total of ~31.3 Mb homology sequences for female *Ch8* were aligned to male *Ch9* with a high identity (~99.0%), representing 83.4% of the whole *Ch8* length (37.5 Mb) (Table S12). Similarly, more than 90.1% of *Ch10* sequences exhibited a high identity with male *Ch9* (Table S12). Meanwhile, approximately 67.0% sequences (63.1 Mb) of the male *Ch9* (94.2 Mb) showed high identity (~99.0%) with those from the female *Ch8* and *Ch10* using nucmer with minimum match length of 1,000 bp (Table S12). After reducing the parameter of minimum match length to 100 bp, we observed that more than 89.5% of the male *Ch9* could align to the female *Ch8* and *Ch10*, suggesting that the male *Ch9* might undergo massive rearrangements during the neo-Y chromosome formation (Table S13 and Figure S5). Indeed, structure variations were identified in sequences for the male *Ch9* lacking homolog to the female *Ch8* and *Ch10*, including 72 breakpoints, 7 translocations, 26 relocations, and 23 inversions (Figure 2C).

According to homology searching of genes in the male genome to the female genome, we identified 172 male-specific genes in the male *Ch9*. Several genes were involved in the chromosome organization and nucleosome assembly processes for fish, such as chromosome transmission fidelity protein 8 (*ctf8*), centromere protein P (*cenpp*), synaptonemal complex protein 1 (*sycp1*), and caveolin 3 (*cav3*) (Table S14). The *ctf8* could regulate sister chromatid cohesion and fidelity of chromosome transmission (Bermudez et al., 2003). The *cenpp* is involved in assembly of kinetochore proteins, mitotic progression, and chromosome segregation (Okada et al., 2006). The *sycp1* is a major component of the transverse filaments of synaptonemal complexes and formed between homologous chromosomes during meiotic prophase (Bisig et al., 2012). The functions of *cav3* could serve as a component of the caveolae plasma membranes in most cell types (Shang et al., 2019).

The conservation synteny analysis for male-female *O. fasciatus* comparison and *O. fasciatus* (the X_1X_2Y system)-*O. latipes* (the normal XY system) comparison using homolog gene pairs between two species were also performed. As a result, twenty-two female *O. fasciatus* chromosomes harbored an excellent

Type	Repbase TEs		TE Proteins		*De Novo*		Combined TEs	
	Length (bp)	% in Genome	Length (bp)	% in Genome	Length (bp)	% in Genome	Length (bp)	% in Genome
DNA	39,085,328	4.92	5,858,619	0.74	83,843,085	10.55	115,535,672	14.53
LINE	24,759,524	3.11	17,460,721	2.20	56,286,293	7.08	85,210,163	10.72
SINE	889,332	0.11	0	0.00	1,986,947	0.25	2,817,685	0.35
LTR	10,536,213	1.33	6,615,817	0.83	32,670,415	4.11	44,682,943	5.62
Satellite	1,910,832	0.24	0	0.00	733,763	0.09	2,480,580	0.31
Simple_repeat	1,304,732	0.16	0	0.00	7,478,505	0.94	8,578,237	1.08
Other	6,957	0.00	171	0.00	0	0.00	7,128	0.00
Unknown	338,847	0.04	0	0.00	30,384,129	3.82	30,719,924	3.86
Total	74,440,379	9.36	29,922,429	3.76	184,141,930	23.16	252,879,666	31.81

Table 3. The Detailed Classification of Repeat Sequences for Male *O. fasciatus*

one-to-one correspondence to those of the male *O. fasciatus* genome except for female C*h8* and C*h10*. The male C*h9* showed strong conserved synteny with female *Ch8* and *Ch10*, consistent with the abovementioned results that *Ch9* might be the neo-Y chromosome (Table S15 and Figures 3, 4, and S6). Furthermore, we found that the synteny of chromosomes for *O. fasciatus* and *O. latipes* was largely conserved. Fourteen chromosomes of male *O. fasciatus* genome were unambiguously aligned to single chromosomes of *O. latipes* genome (Table S15 and Figure 4). Other nine chromosomes of the male *O. fasciatus* genome exhibited several small inter-chromosome conservation synteny to *O. latipes* chromosomes, suggesting that massive inter-chromosome rearrangements occurred after divergence of two species (Table S15 and Figure 4). We found that *Ch5* and *Ch6* in the *O. latipes* genome exhibited excellent synteny with female *Ch8* and *Ch10*, as well as with *Ch9* of male *O. fasciatus* (Table S15 and Figures 4 and S6).

The syntenic blocks of the chromosomes were also evaluated among the male/female *O. fasciatus* and *L. crocea* genomes using the program MUMmer. The consistency of chromosomes, with 24 blocks between female *O. fasciatus* and *L. crocea* and 23 blocks among male *O. fasciatus*, *L. crocea,* and female *O. fasciatus*, was detected (Figure 3). Precise pairings of protein-coding genes originating from the male and female *O. fasciatus* chromosomes were established using BLASTP software with identity $\geq$95% (coverage $\geq$90%) and e-value $\leq 1 \times 10^{-5}$. The results showed that 10,919 protein-coding gene pairs were identified, 1,459 of which were located on the large neo-chromosome (*Ch9*) in the male genome, corresponding to 809 genes of *Ch8* and 628 genes of *Ch10* in the female genome (Figure 3).

Gene Family Identification and Phylogenetic Tree Construction

According to the homolog searching of protein-coding genes for male *O. fasciatus* and other species, including *Salmo salar*, *L. crocea*, *G. morhua*, *P. olivaceus*, *C. semilaevis*, *Nolothenia coriiceps*, *Boleophthalmus pectinirostris*, *Branchiostoma floridae*, *G. aculeatus*, *Callorhinchus milii*, *Danio rerio* and *O. latipes*, approximately 23,302 gene families were identified based on their H-scores (Figure S7). The specific and common gene families of male *O. fasciatus* and other teleosts (*L. crocea*, *G. morhua,* and *S. salar*) were further analyzed, which yielded 551 specific gene families in the male genome and 11,484 common gene families among the four teleosts (Figure S8). Using the MCL program implemented in the OrthoMCL pipeline with a coefficient setting of 1.5 to cluster the abovementioned gene families, we obtained 810 single-copy genes, which were employed to reconstruct the phylogenetic relationships among male *O. fasciatus* and the other species. Based on a length filter that retained protein sequences $\geq$100 amino acids, 759 single-copy orthogroups were obtained using ClustalW software to extract and align single-copy genes from the 810 single-copy orthogroups (Figure S7). The multiple sequence alignment for the filtered single-copy genes was performed using MUSCLE software, and a super-alignment dataset for each species was obtained and used to construct a phylogenetic tree of the male *O. fasciatus* and the other species based on the maximum-likelihood method implemented in the RAxML package (Figure 5). The results of the phylogenetic tree showed that *O. fasciatus* from the Oplegnathidae family of the Centrarchiformes (Eupercaria) was close to *L. crocea* in the order Perciformes (Eupercaria), consistent with the new

Type		Number	Percent (%)
Total		24,835	
Annotated	InterPro	21,696	87.36
	GO	16,494	66.41
	KEGG_ALL	23,916	96.30
	KEGG_KO	15,260	61.45
	Swissprot	22,380	90.11
	TrEMBL	23,953	96.45
	NR	24,072	96.93
Annotated		24,105	97.06
Unannotated		730	2.94

Table 4. Functional Annotation of the Protein-Coding Genes in Male *O. fasciatus* Genome

phylogenetic classification of bony fishes (Figure 5) (Betancur-R et al., 2017). The divergence times among clades were evaluated using the MCMCtree program with calibration times based on the TimeTree database, showing that *O. fasciatus* diverged from its common ancestor with *L. crocea* approximately 62.8–73.4 million years ago (Figure 5).

DISCUSSION

O. fasciatus is an important fishery species in offshore cage aquaculture and fish stocking for marine ranching in East Asia (Schembri et al., 2010; Xiao et al., 2016, 2019). The male *O. fasciatus* genome was characterized by an X_1X_2Y system with a neo-Y chromosome based on male karyotype analyses. The species could be used as an excellent model to address the sex determination, origin, and evolution of the X_1X_2Y system. The chromosome-level genome of male *O. fasciatus* assembled in the present study, combined with the released reference genome of female *O. fasciatus*, will provide valuable genomic resources to gain insights into the origin of the X_1X_2Y system (Xiao et al., 2019).

To assess the quality of the assembly, the continuity and completeness of the genome was evaluated. The final contig assembly was 795.1 Mb with a contig N50 length of 2.13 Mb for male *O. fasciatus*, which was comparable to those of the female (Xiao et al., 2019). The contig N50 values of the male/female *O. fasciatus* genomes were also larger than those of many reported teleost genomes, which indicated that high genome continuity existed in *O. fasciatus* genomes (Table S3); 1,355 ordered contigs were scaffolded into 23 chromosomes, yielding a final chromosome-level genome of approximately 762 Mb with a scaffold N50 length of 32.43 Mb (Table 1). The completeness of the assembled genome was evaluated using BUSCO. The high continuity and completeness of the male *O. fasciatus* genome will lay a solid foundation for further studies of population genetics, evolutionary of genome comparisons, neo-chromosome structure, and sex-determining mechanisms (Sun et al., 2017, 2019; Yang et al., 2018).

So far, 37 species have been reported to possess multiple sex chromosomes with $X_1X_1X_2X_2/X_1X_2Y$ system among teleosts. Although techniques, such as Giemsa staining, C-banding, repetitive DNA markers, CGH and WCP, have been used for chromosomal studies, the origination of the neo-Y chromosome of *O. fasciatus* in previous studies was still largely hindered by the lack of reference genome resources, especially for the neo-Y chromosome (Sember et al., 2015; Bitencourt et al., 2016; Zhang et al., 2018; Krysanov and Demidova, 2018; Cai et al., 2019; Xu et al., 2019). In this work, a large neo-chromosome (*Ch9*) was assembled into 94.2 Mb, corresponding to the large metacentric Y chromosome of male *O. fasciatus*. The neo-chromosome could be responsible for the genome size discrepancy between male and female *O. fasciatus* (Table S4 and Figure 1).

Three proposed mechanisms for the origin of an X_1X_2Y multiple sex chromosome system have been postulated, which included fusion between the Y chromosome and an autosome, fission of the X chromosome, and reciprocal translocation between the X chromosome and an autosome (White, 1983; Kitano and Peichel, 2012). All those

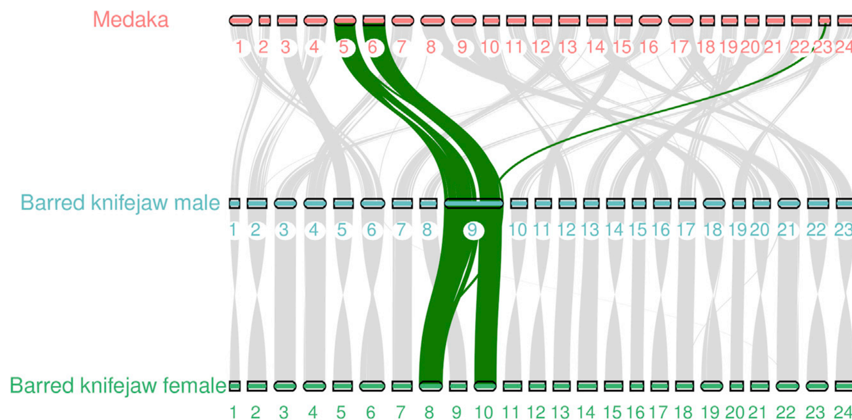

Figure 4. Chromosome Conserved Synteny between *Oryzias latipes* Genome (the Normal XY system) and *O. fasciatus* Genome (the X_1X_2Y System)

Ribbons between two genomes represented chromosomal conservation synteny blocks.

mechanisms (fusion and fission) could induce remarkable genome size changes for sex chromosomes (Y, X), leading to a large neo-Y chromosome or a small neo-X chromosome (Kitano and Peichel, 2012). Previous studies have shown that the X_1X_2Y systems of teleosts mainly originate from chromosomal fusions, leading to large metacentric chromosomes (neo-Y chromosomes) through a Robertsonian fusion of two acrocentric chromosomes (the Y chromosome and an autosome) (Uyeno and Miller, 1971; Bertollo et al., 2000, 2004; Ueno and Takai, 2008; Kitano and Peichel, 2012). Although the formation of the X_1X_2Y multiple sex chromosome system could be achieved through fission of the X chromosome, this process would lead to an increase in the diploid number of chromosomes (e.g., female 2n = 50, male 2n = 49) compared with the ancestral karyotype of marine teleost (2n = 48) (White, 1983; Kitano and Peichel, 2012). Our genome assembly for males and females of *O. fasciatus* led to 23 and 24 chromosomes, directly corresponding to the male and female karyotypes (2n = 47/48), respectively (Figures 1 and 2) (Xu et al., 2012; Xiao et al., 2019). The comparative analysis showed excellent chromosomal synteny between the male and female *O. fasciatus* genomes (Figures 1, 2, and 3). No small neo-X chromosome was observed at the genome level; however, a large neo-Y chromosome (*Ch9*) (63.1 Mb/94.2 Mb) in the male *O. fasciatus* genome exhibited high identity (~99.0%) to those of the female chromosomes *Ch8* and *Ch10*. From the chromosomal comparison, *O. fasciatus* female *Ch8* and *Ch10* exhibited excellent synteny with those of *Ch5* and *Ch6* in *O. latipes* genome, indicating *Ch8* and *Ch10* in *O. fasciatus* likely separated in their common ancestor (Table S12). According to the sequence and synteny comparison and previous karyotypes results, we suggested that a centric fusion of acrocentric chromosomes *Ch8* and *Ch10* should be responsible for the formation of the X_1X_2Y system of male *O. fasciatus*.

Neo-sex chromosome systems are always derived from rearrangements between original sex chromosomes and autosomes through chromosomal fissions, fragmentations, and fusions (Uyeno and Miller, 1971; Bertollo et al., 2000, 2004; Ueno and Takai, 2008; Kitano and Peichel, 2012). Indeed, although the male large neo-chromosome *Ch9* showed general excellent synteny with the female *Ch8*/*Ch10*, several obvious rearrangements were also observed at the middle of the chromosomes between *Ch9* and *Ch8*/*Ch10*, especially for flanking regions of breakpoints around 18 Mb–20 Mb, 28 Mb–32 Mb, and 39 Mb–47 Mb in male *Ch9* (Figure 2). Cross-chromosome synteny was also identified between the male *Ch9* of *O. fasciatus* and the *Ch5*/*Ch6* of *O. latipes* genome, which exhibited excellent synteny with female *Ch8* and *Ch10* of *O. fasciatus* (Figure 4). These results showed that chromosome rearrangements events have occurred in the neo-chromosome *Ch9* of male *O. fasciatus*.

The neo-chromosomes of the X_1X_2Y system could also participate in sex regulation and determination (Ueno and Takai, 2008). Previous studies showed that neo-chromosomes might harbor important genes or regulatory elements responsible for the behaviors, phenotype, and speciation (Kitano et al., 2009). Some male-specific genes involved in chromosome and nucleosome assembly (*ctf8*, *cenpp*, *sycp1*) and steroid hormone synthesis (*nr4a1*) were identified in the present study, which might be responsible for the fidelity of homologous chromosome pairing between *Ch9* and *Ch8*/*Ch10* during meiotic prophase and male sex determination (Table S14). This high-quality chromosome-level genome will enable us to explore the fusion mechanism and biological functions of neo-chromosomes by analyses of the genetic composition

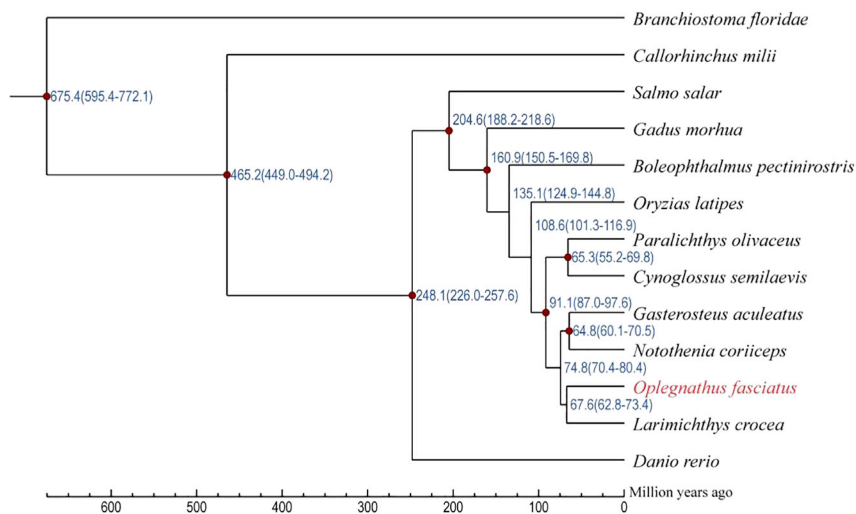

Figure 5. Phylogenetic Analysis of Male *O. fasciatus* and Other Related 12 Species

A total of 21,528 gene families were identified by clustering the homologous gene sequences, and 810 single-copy orthogroups were obtained; 719 filtered single-copy orthogroups were used to construct the phylogenetic relationship between *O. fasciatus* and other species (*S. salar*, *L. crocea*, *G. morhua*, *P. olivaceus*, *C. semilaevis*, *N. coriiceps*, *B. pectinirostris*, *B. floridae*, *G. aculeatus*, *C.milii*, *D. rerio*, and *O. latipes*). Divergence times among the species (red dots) from TimeTree database were used as the calibration divergence times. Blue values on branches indicated the estimated divergence time in millions of years ago (Mya), and numbers in parentheses showed the interval of 95% confidence.

and chromosome conformation studies based on the Hi-C. The multiple sex chromosome system with sexual dimorphism could also lead to growth differences. Sexual dimorphism in growth has been detected in *O. fasciatus*—male fish grow faster than females (Chen et al., 2014; Xiao, 2015). A total of 24,105 protein-coding genes were functionally annotated for the chromosome-level genome of male *O. fasciatus*, and these genes will serve as a framework combined with quantitative trait locus (QTL) and bulked segregant analysis (BSA) techniques for studies of growth regulation and breeding.

In summary, we have successfully completed a chromosome-level genome assembly for male *O. fasciatus* and first assembled the large neo-chromosome corresponding to the karyotype of male *O. fasciatus* with high continuity and completeness. This study demonstrated for the first time that the X_1X_2Y system of male *O. fasciatus* originated from the fusions of the non-homologous chromosomes *Ch8* and *Ch10* via significant homology and chromosomal interactions at the genome level. This high-quality genome assembly will not only provide a solid foundation for further sex-determining mechanism research in the X_1X_2Y system but also facilitate the artificial breeding aiming to improve the yield and disease resistance for *Oplegnathus*.

Limitations of the Study

Chromosome fusion was suggested to be responsible for the formation of the X_1X_2Y system only from the male *O. fasciatus*; the extremely limited genome information of the fishes with multiple sex chromosomes led to difficulties in accurately determining the dynamics and mechanism of chromosome fusions.

METHODS

All methods can be found in the accompanying Transparent Methods supplemental file.

DATA AND CODE AVAILABILITY

The RNA sequencing data of the *Oplegnathus fasciatus* have been deposited in the SRA under Bioproject number PRJNA486572. The whole-genome sequencing data are available in the NBCI with the accession number SRP220007.

SUPPLEMENTAL INFORMATION

Supplemental Information can be found online at https://doi.org/10.1016/j.isci.2020.101039.

ACKNOWLEDGMENTS

This study was supported by a grant from the National Natural Science Foundation of China (No. 41506170, No. 31672672, and No. 31872195), National Key Research and Development Program (2018YFD0901204), STS project (KFZD-SW-106, ZSSD-019, 2017T3017, KFJ-STS-QYZX-020), Qingdao National Laboratory for Marine Science and Technology (2018SDKJ0502-2, 2015ASKJ02), China Agricultural Research System (CARS-47), Shandong Province Key Research and Invention Program (2017GHY15102, 2017GHY15106), Qingdao Source Innovation Program (17-1-1-57-jch), Marine Fishery Institute of Zhejiang Province, and Key Laboratory of Mariculture and Enhancement of Zhejiang Province (2016KF002). The project of Guangdong laboratory of southern ocean science and engineering (GML2019ZD0402).

AUTHOR CONTRIBUTIONS

Y.X. conceived the project. Z.X., D.M., Jun Li collected the samples and extracted the genomic DNA. Y.X., Jing Liu, C.Z., H.W., L.L., W.N., S.X., and Jun Li performed the genome assembly and data analysis. Y.X., Z.X., S.X., Jing Liu, D.M., and Jun Li wrote the paper. A.H.-U. polished the paper.

DECLARATION OF INTERESTS

The authors declare no competing interests.

Received: December 11, 2019
Revised: March 5, 2020
Accepted: April 1, 2020
Published: April 24, 2020

REFERENCES

Bertollo, L.A.C., Born, G.G., Dergam, J.A., Fenocchio, A.S., and Moreira-Filho, O. (2000). A biodiversity approach in the neotropical Erythrinidae fish, *Hoplias malabaricus*. Karyotypic survey, geographic distribution of cytotypes and cytotaxonomic considerations. Chromosome Res. *8*, 603–613.

Bertollo, L.A.C., Oliveira, C., Molina, W.F., Margarido, V.P., Fontes, M.S., Pastori, M.C., and Fenocchio, A.S. (2004). Chromosome evolution in the erythrinid fish, *Erythrinus erythrinus* (Teleostei: Characiformes). Heredity *93*, 228–233.

Betancur-R, R., Wiley, E.O., Arratia, G., Acero, A., Bailly, N., Miya, M., Lecointre, G., and Ortí, G. (2017). Phylogenetic classification of bony fishes. BMC Evol. Biol. *17*, 162.

Bitencourt, J.A., Sampaio, I., Ramos, R.T.C., Vicari, M.R., and Affonso, P.R.A.M. (2016). First report of sex chromosomes in Achiridae (Teleostei: Pleuronectiformes) with inferences about the origin of the multiple $X_1X_1X_2X_2/X_1X_2Y$ system and dispersal of ribosomal genes in *Achirus achirus*. Zebrafish *14*, 90–95.

Blanco, D.R., Vicari, M.R., Lui, R.L., Bertollo, L.A.C., Traldi, J.B., and Moreira-Filho, O. (2013). The role of the Robertsonian rearrangements in the origin of the XX/XY_1Y_2 sex chromosome system and in the chromosomal differentiation in *Harttia* species (Siluriformes, Loricariidae). Rev. Fish Biol. Fisher *23*, 127–134.

Bermudez, V.P., Maniwa, Y., Tappin, I., Ozato, K., Yokomori, K., and Hurwitz, J. (2003). The alternative Ctf18-Dcc1-Ctf8-replication factor C complex required for sister chromatid cohesion loads proliferating cell nuclear antigen onto DNA. Proc. Natl. Acad. Sci. U S A *100*, 10237–10242.

Bisig, C.G., Guiraldelli, M.F., Kouznetsova, A., Scherthan, H., Höög, C., Dawson, D.S., and Pezza, R.J. (2012). Synaptonemal complex components persist at centromeres and are required for homologous centromere pairing in mouse spermatocytes. PLoS Genet. *8*, e1002701.

Cai, M.Y., Xiao, S.J., Li, W.B., Han, Z.F., Han, F., Xiao, J.Z., Liu, F.L., and Wang, Z.Y. (2019). Chromosome assembly of *Collichthys lucidus*, a fish of Sciaenidae with a multiple sex chromosome system. Sci. Data *6*, 132.

Chen, S.L., Zhang, G.J., Shao, C.W., Huang, Q.F., Liu, G., Zhang, P., Song, W.T., An, N., Chalopin, D., Volff, J.N., et al. (2014). Whole-genome sequence of a flatfish provides insights into ZW sex chromosome evolution and adaptation to a benthic lifestyle. Nature *46*, 253–260.

Cioffi, M.B., and Bertollo, L.A.C. (2012). Chromosomal distribution and evolution of repetitive DNAs in fish. Repetit. DNA *7*, 197–221.

Ferreira, M., Garcia, C., Matoso, D.A., de Jesus, I.S., and Feldberg, E. (2016). A new multiple sex chromosome system X1X1X2X2/X1Y1X2Y2 in Siluriformes: cytogenetic characterization of *Bunocephalus coracoideus* (Aspredinidae). Genetica *144*, 591–599.

Kitano, J., and Peichel, C. (2012). Turnover of sex chromosomes and speciation in fishes. Environ. Biol. Fish. *94*, 549–558.

Kitano, J., Ross, J.A., Mori, S., Kume, M., Jones, F.C., Chan, Y.F., Absher, D.M., Grimwood, J., Schmutz, J., Myers, R.M., et al. (2009). A role for a neo-sex chromosome in stickleback speciation. Nature *461*, 1079–1083.

Koren, S., Walenz, B.P., Berlin, K., Miller, J.R., Bergman, N.H., and Phillippy, A.M. (2017). Canu: scalable and accurate long-read assembly via adaptive *k*-mer weighting and repeat separation. Geneome Res. *27*, 722–736.

Krysanov, E., and Demidova, T. (2018). Extensive karyotype variability of African fish genus Nothobranchius (Cyprinodontiformes). Comp. Cytogenet. *12*, 387–402.

Li, H., Sun, Z.P., Li, Q., and Jiang, Y.L. (2011). Characterization of an iridovirus detected in rock bream (*Oplegnathus fasciatus*; Temminck and Schlegel). Chin. J. Virol. *27*, 158–164.

Okada, M., Cheeseman, I.M., Hori, T., Okawa, K., McLeod, I.X., Yates, J.R., Desai, A., and Fukagawa, T. (2006). The CENP-H-I complex is required for the efficient incorporation of newly synthesized CENP-A into centromeres. Nat. Cell Biol. *8*, 446–457.

Parise-Maltempi, P.P., Martins, C., Oliveira, C., and Foresti, F. (2007). Identification of a new repetitive element in the sex chromosomes of *Leporinus elongatus* (Teleostei: Characiformes: Anostomidae): new insights into the sex chromosomes of *Leporinus*. Cytogenet. Genome Res. *116*, 218–223.

Park, H.S., Kim, C.G., Kim, S., Park, Y.J., Choi, H.J., Xiao, Z.Z., Li, J., Xiao, Y.S., and Lee, Y.H. (2018). Population genetic structure of rock bream (*Oplegnathus fasciatus* Temminck & Schlegel, 1844) revealed by mtDNA COI sequence in Korea and China. Ocean. Sci. J. *53*, 261–274.

Schembri, P.J., Bodilis, P., Evans, J., and Francour, P. (2010). Occurrence of barred kinfejaw, *Oplegnathuf fasciatus* (Actinopterygii: Perciformes: Oplegnathidae), in Malta (Central Mediterranean) with a discussion on possible modes of entry. Acta Ichthyol. Piscat. *40*, 101–104.

Sember, A., Bohlen, J., Šlechtová, V., Altmanová, M., Symonová, R., and Ráb, P. (2015). Karyotype differentiation in 19 species of river loach fishes (Nemacheilidae, Teleostei): Extensive variability associated with rDNA and heterochromatin distribution and its phylogenetic and ecological interpretation. BMC Evol. Biol. *15*, 251–272.

Simão, F.A., Waterhouse, R.M., Ioannidis, P., Kriventseva, E.V., and Zdobnov, E.M. (2015). BUSCO: assessing genome assembly and annotation completeness with single-copy orthologs. Bioinformatics *31*, 3210–3212.

Shang, L., Chen, T., Xian, J., Deng, Y., Huang, Y., Zhao, Q., Liang, G., Liang, Z., Lian, F., Wei, H., and Huang, Q. (2019). The caveolin-3 P104L mutation in LGMD-1C patients inhibits non-insulin-stimulated glucose metabolism and growth but promotes myocyte proliferation. Cell Biol. Int. *43*, 669–677.

Sun, J., Zhang, Y., Xu, T., Zhang, Y., Mu, H., Zhang, Y., Lan, Y., Fields, C.J., Hui, J.H.L., Zhang, W., et al. (2017). Adaptation to deep-sea chemosynthetic environments as revealed by mussel genomes. Nat. Ecol. Evol. *1*, 121.

Sun, J., Mu, H.W., CH Ip, J., Li, R.S., Xu, T., Accorsi, A., Sánchez Alvarado, A., Ross, E., Lan, Y., Sun, Y.N., et al. (2019). Signatures of divergence, invasiveness, and terrestrialization revealed by four apple snail genomes. Mol. Biol. Evol. *36*, 1507–1520.

Temminck, C.J., and Schlegel, H. (1844). In: P.F. von Siebold. Fauna Japonica. P, 62.

Ueno, K., and Takai, A. (2008). Multiple sex chromosome system of $X_1X_1X_2X_2/X_1X_2Y$ type in lutjanid fish, *Lutjanus quinquelineatus* (Perciformes). Genetica *132*, 35–41.

Uyeno, T., and Miller, R.R. (1971). Multiple sex chromosomes in a Mexican Cyprinodontid fish. Nature *231*, 452–453.

Walker, B., Abeel, T., Shea, T., Priest, M., Abouelliel, A., Sakthikumar, S., Cuomo, C.A., Zeng, Q.D., Wortman, J., Yong, S.K., et al. (2014). Pilon: an integrated tool for comprehensive microbial variant detection and genome assembly improvement. PLoS one *9*, e112963.

White, M.J.D. (1983). Animal Cytology and Evolution (Cambridge University Press).

Xiao, Y.S., Li, J., Ren, G.J., Ma, G.Y., Wang, Y.F., Xiao, Z.Z., and Xu, S.H. (2016). Pronounced population genetic differentiation in the rock bream *Oplegnathus fasciatus* inferred from mitochondrial DNA sequences. Mitochondrial DNA A DNA Mapp. Seq. Anal. *27*, 2045–2052.

Xiao, Y.S., Xiao, Z.Z., Ma, D.Y., Liu, J., and Li, J. (2019). Genome sequence of the barred knifejaw Oplegnathus fasciatus (Temminck & Schlegel, 1884): the first chromosome-level draft genome in the family Oplegnathidae. GigaScience *8*, giz013.

Xiao, Z.Z. (2015). Study on Population Genetics and Culture Biology of *Oplegnathus fasciatus* Doctor thesis (China National Knowledge Internet), pp. 162–176.

Xu, D.D., Sember, A., Zhu, Q.H., de Oliveira, E.A., Liehr, T., Al-Rikabi, A.B.H., Xiao, Z.Z., Song, H.B., and de Bello Cioffi, M. (2019). Deciphering the origin and evolution of the X_1X_2Y system in two Closely-related *Oplegnathus* species (Oplegnathidae and Centrarchiformes). Int. J. Mol. Sci. *20*, 3571.

Xu, D.D., You, F., Lou, B., Geng, Z., Li, J., and Xiao, Z.Z. (2012). Comparative analysis of karyotype and C-banding in male and female Oplegnathus fasciatus. Acta Hydrobiol. Sin. *36*, 552–557.

Xue, R., An, H., Liu, Q.H., Xiao, Z.Z., Wang, Y.F., and Li, J. (2016). Karyotype and Ag-NORs in male and female of *Oplegnathus punctatus*. Oceanol. Limnol. Sin. *47*, 626–632.

Yang, X.F., Liu, H.P., Ma, Z.H., Zou, Y., Zou, M., Mao, Y.Z., Li, X.M., Wang, H., Chen, T.S., and Wang, W.M. (2018). Chromosome-level genome assembly of *Triplophysa tibetana*, a fish adapted to the harsh high-altitude environment of the Tibetan Plateau. Mol. Ecol. Resour. *19*, 1027–1036.

Zhang, B.C., Zhang, J., Xiao, Z.Z., and Sun, L. (2014). Rock bream (*Oplegnathus fasciatus*) viperin is a virus-responsive protein that modulates innate immunity and promotes resistance against megalocytivirus infection. Dev. Comp. Immunol. *45*, 35–42.

Zhang, S., Zheng, J., Zhang, J., Wang, Z.Y., Wang, Y., and Cai, M. (2018). Cytogenetic characterization and description of an $X_1X_1X_2X_2/X_1X_2Y$ sex chromosome system in *Collichthys lucidus* (Richardson, 1844). Acta Oceanol. Sin. *37*, 34–39.

iScience, Volume *23*

Supplemental Information

Chromosome-Level Genome Reveals the Origin of Neo-Y Chromosome in the Male Barred Knifejaw *Oplegnathus fasciatus*

Yongshuang Xiao, Zhizhong Xiao, Daoyuan Ma, Chenxi Zhao, Lin Liu, Hao Wu, Wenchao Nie, Shijun Xiao, Jing Liu, Jun Li, and Angel Herrera-Ulloa

Supplemental Figures

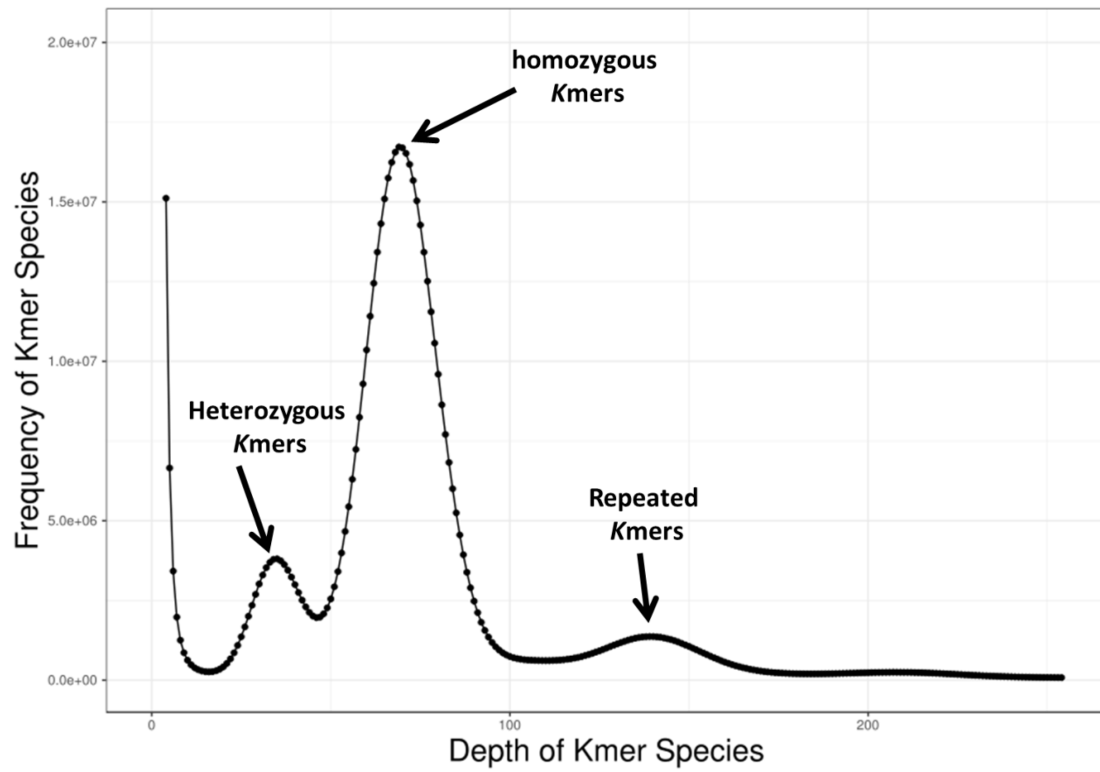

Figure S1. *K*-mer distribution of male *O. fasciatus* genome, Related to Table 1.

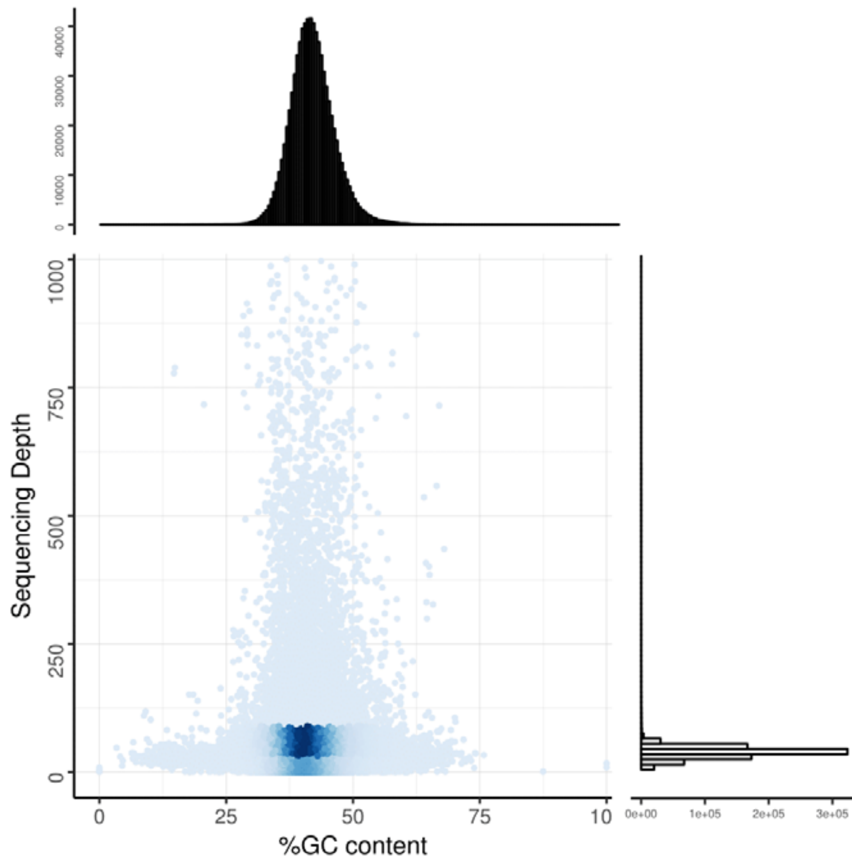

Figure S2. The GC content of male *O. fasciatus* base on the PacBio platform for genome assembly GC statistics based on the CLR (continuous long reads) mapping information using a sliding window approach (10kb windows), Related to Table 1.

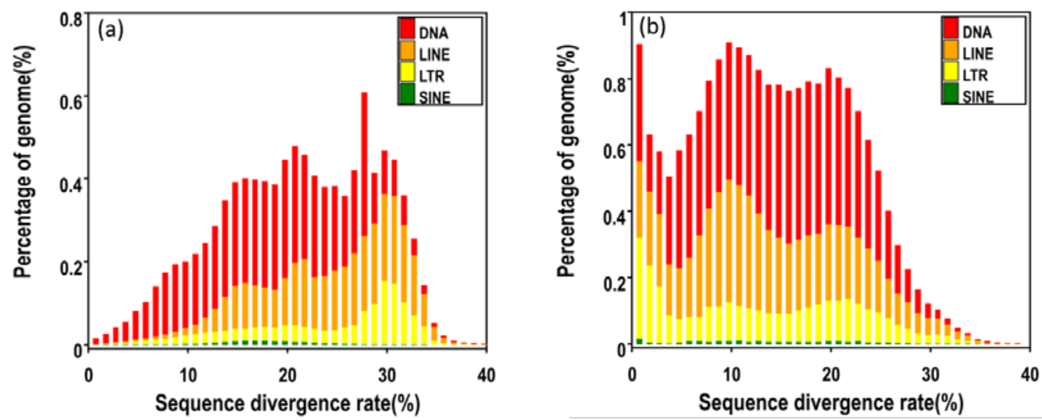

Figure S3. Interspersed repeats statistics of genome assembly for male *O. fasciatus*. (a) Repbase library, (b) *de novo* library, Related to Table 2 and Table 3.

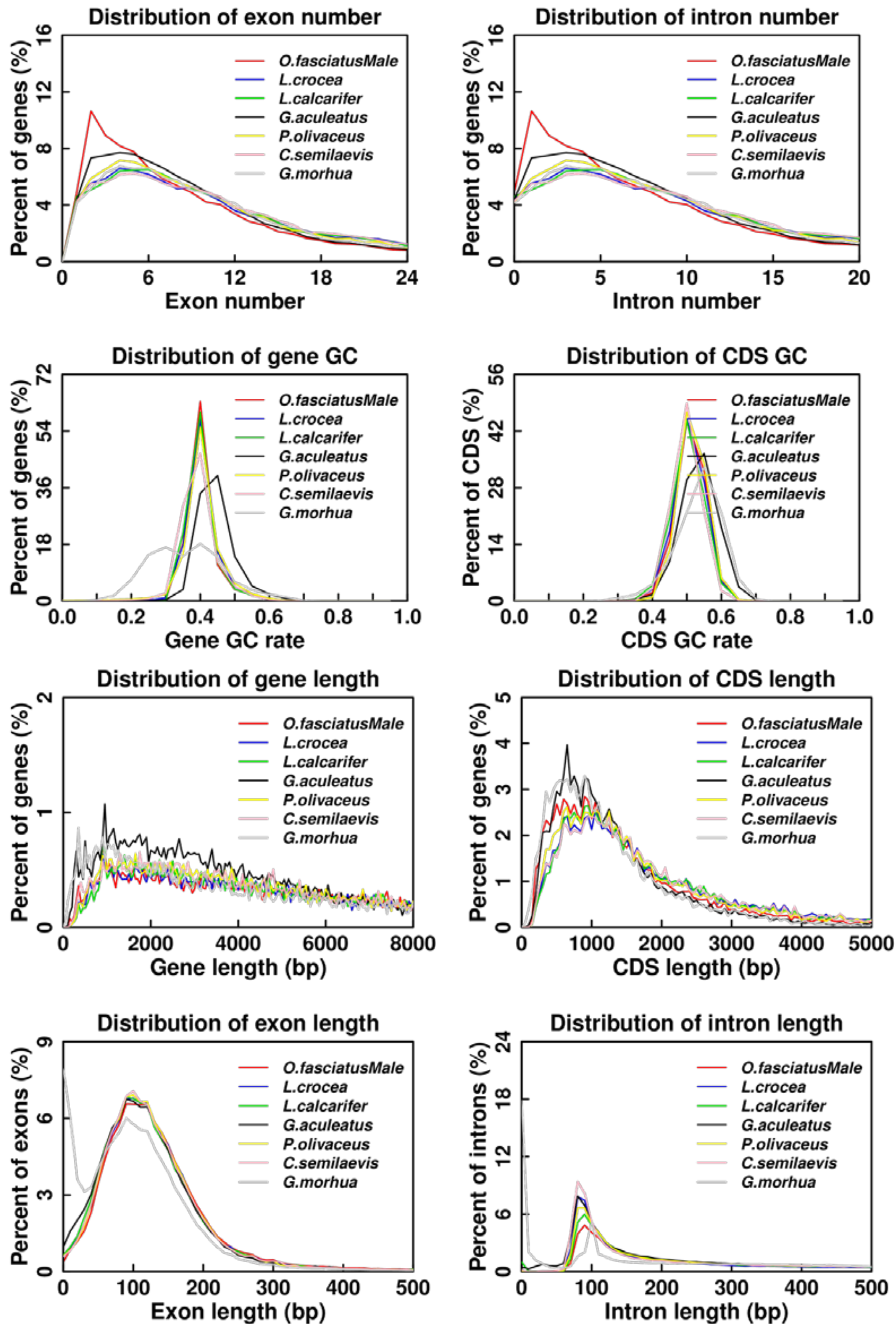

Figure S4. The gene number, GC content, gene length distribution, CDS length distribution, exon length distribution and intron length distribution for male *O. fasciatus* were all comparable with those in other teleost fish species (*Larimichthys crocea*，*Lates calcarifer*, *Gasterosteus aculeatus*, *Paralichthys olivaceus*, *Cynoglossus semilaevis* and *Gadus morhua*), Related to Table 1 and Table 2.

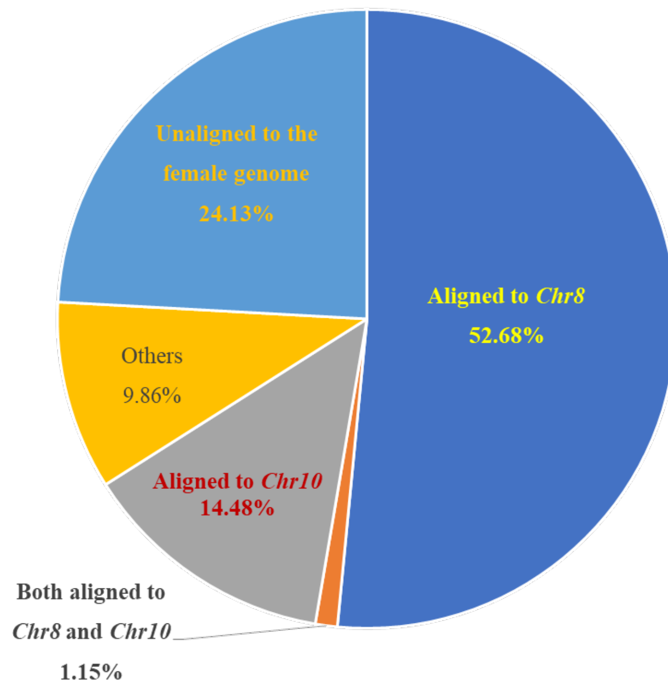

Figure S5. Distribution of the rest chromosomal sequences of the male *Ch9* compared to the whole female genome of *O. fasciatus*, Related to Figure 3 and Table S13.

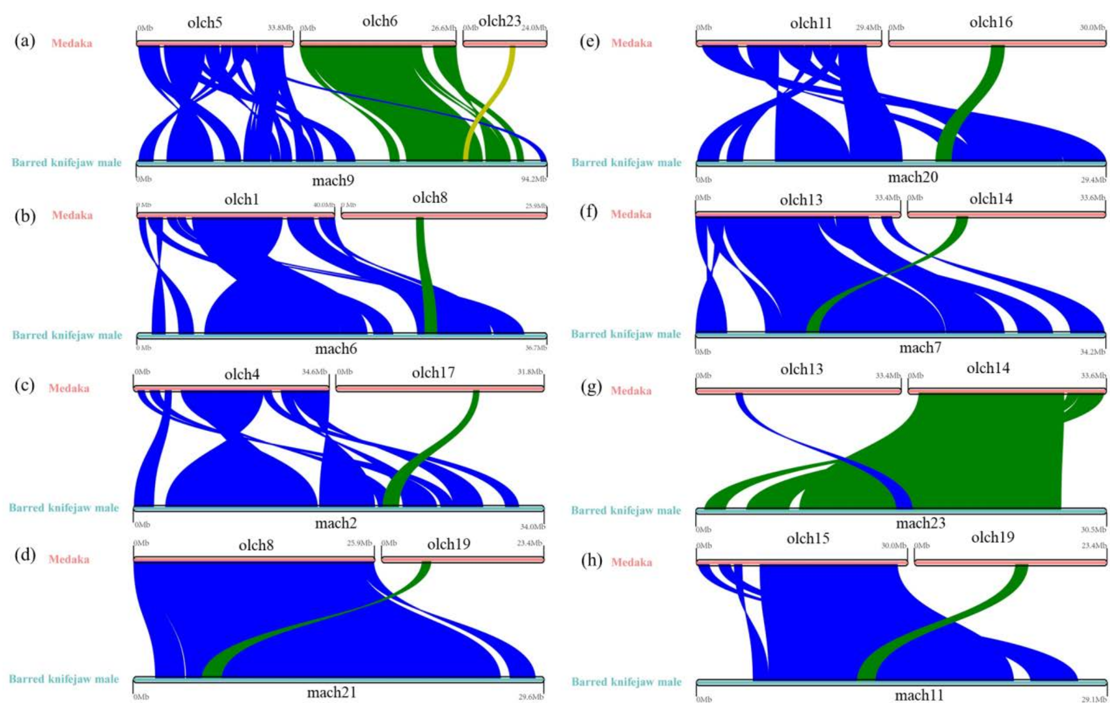

Figure S6. (a)-(h) Chromosome conserved synteny with one-to-two or one-to-three collinear alignment relationships between *Oryzias latipes* (the normal XY system) and *O. fasciatus* (the X_1X_2Y system), Related to Figure 4 and Table S15..

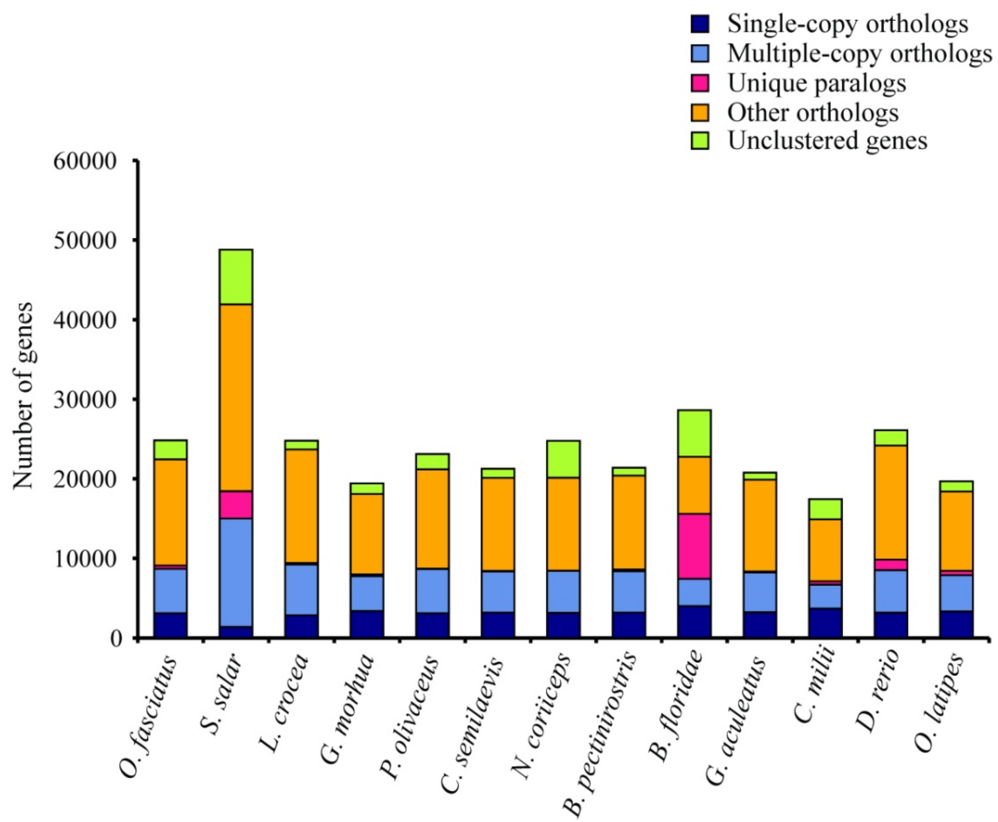

Figure S7. Comparing genome assemblies between male *O. fasciatus* and other 12 species, Related to Figure 5.

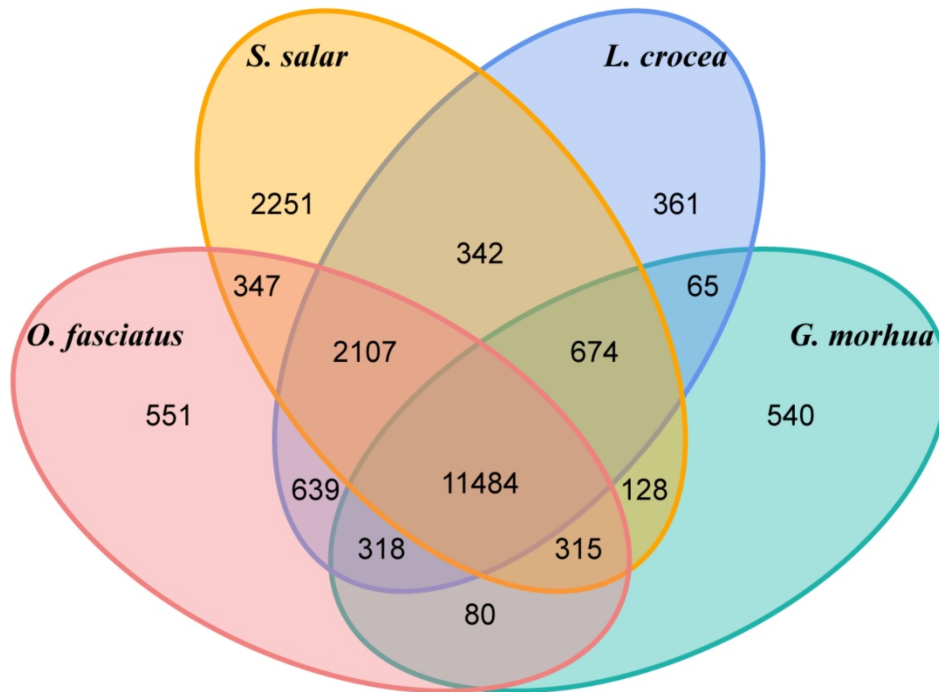

Figure S8. The Venn Diagram of orthologous gene families between male *Oplegnathus fasciatus* and the other four fish genomes (*Larimichthys crocea*, *Gadus morhua* and *Salmo salar*), Related to Figure 5 and Table 4.

Supplemental Tables

Table S1. Summary of sequence data from male *O. fasciatus*, Related to Figure 1 and Table 1.

Type	Method	Library size (bp)	Data size (Gb)	Read N50 (bp)
DNA	HiSeq 2000	300~350	63.9	150
DNA	PacBio Sequel	22,000	39.8	18,850
DNA (Hi-C)	HiSeq 2000	300~350	95.9	150
RNA	HiSeq 2000	150	42.2	150

Table S2. Genome assembly statistics for male *O. fasciatus*, Related to Figure 1, Figure 2, Figure 3 and Table 1.

Method	Type	Genome size (Mb)	Longest sequence (Mb)	Sequences number	Sequence N50 (Mb)
Canu	Contig	866.9	9.820	4,453	1.7331
Redundans	Contig	794.8	9.820	2,295	2.1271
Smrtlink	Contig	794.8	9.820	2,295	2.1271
Pilon	Contig	795.1	9.825	2,295	2.1271
Final	Contig	795.1	9.825	2,295	2.1271

Table S3. Comparing genome assemblies between *O. fasciatus* and other fish species

Some data were cited from the reference, Related to Figure 5 and Table 1.

Species	**Estimated Genome Size (Mb)**	**Contig N50 (Mb)**	**Scaffold N50 (Mb)**
***Oplegnathus fasciatus* male**	795	2.13	32.43
***Oplegnathus fasciatus* female**	768	2.13	33.55
Larimichthys crocea*	679	0.06	1.03
Ictalurus punctatus*	845	0.05	7.20
Paralichthys olivaceus*	546	0.03	3.90
Hippocampus comes*	501	0.04	1.80
Gadus morhua*	643	0.12	1.15
Channa argus*	615	0.08	4.50
Anguilla rostrata*	1,410	0.01	0.086
Anguilla anguilla*	860	0.001	0.077
Lates calcarifer*	700	1.06	25.80
Clupea harengus*	850	0.02	1.84
Scophthalmus maximus*	568	0.03	4.30
Miichthys miiuy*	636	0.07	1.15
Lepisosteus oculatus*	945	0.07	6.90
Sillago sinica	534	2.60	-
Lates calcarifer*	586	1.07	25.85
Oreochromis niloticus*	868	3.30	37.00

* The data was cited from the reference Gong et al., 2018.

Table S4. Aligment of clean reads for Hi-C data and Hi-C libraries for chromosome-scale assembly, Related to Figure 1, Figure 2, Figure 3 and Table 1.

Clean data		650,652,366	
Paired		621,961,380 (95.59%)	
With mate mapped to a different contig (or scaffold)		235,931,390 (37.93%)	
With mate mapped to a different contig (or scaffold) (map Q⩾5)		202,370,680 (32.54%)	
Chromosome	Number of contigs	Length of contigs	Length of chromosome
Chr1	27	19,038,723	19,051,723
Chr2	35	34,023,620	34,040,620
Chr3	31	32,802,329	32,817,329
Chr4	50	33,465,990	33,490,490
Chr5	35	37,834,216	37,851,216
Chr6	50	36,641,980	36,666,480
Chr7	48	34,194,075	34,217,575
Chr8	31	30,421,100	30,436,100
Chr9	444	94,021,031	94,242,531
Chr10	42	29,231,680	29,252,180

Chr11	33	29,145,809	29,161,809
Chr12	50	32,406,821	32,431,321
Chr13	75	28,647,297	28,684,297
Chr14	34	28,866,314	28,882,814
Chr15	47	27,458,915	27,481,915
Chr16	30	27,627,606	27,642,106
Chr17	43	25,918,704	25,939,704
Chr18	36	33,054,315	33,071,815
Chr19	33	24,737,159	24,753,159
Chr20	54	29,419,855	29,446,355
Chr21	40	29,573,728	29,593,228
Chr22	57	32,586,236	32,614,236
Chr23	30	30,484,110	30,498,610
Total	1,355	761,601,613	762,267,613

Table S5. The completeness and coverage statistics of genome assembly for male *O. fasciatus* using CLR mapping information, Related to Table 2.

Mapping rate (%)	**Average sequencing depth**	**Coverage (%)**	**Coverage (≥5X, %)**	**Coverage (≥10X, %)**	**Coverage(≥20X, %)**
87.63	50.05	99.89	99.55	98.94	94.24

Table S6. The accuracy estimation of genome assembly for male *O. fasciatus* based on SNP calling, Related to Table 2.

SNP	**Number**	**Percentage of SNP (%)**	**Percentage of genome (%)**
All SNP	1,873,725	100.00	0.24
Heterozygosis SNP	1,863,418	99.45	0.23
Homology SNP	10,307	0.55	0.00
All indel	608,220	100.00	0.08
Heterozygosis indel	573,975	94.37	0.07
Homology indel	34,245	5.63	0.00

Table S7. Repeat content comparison of male *O. fasciatus* with several other teleost, Related to Table 3 and Figure S3.

	Gasterosteus aculeatus	***Larimichthys crocea***	***Oryzias latipes***	***Dicentrarchus labrax***	***Triplophysa tibetana***	***Epinephelus lanceolatus***	***Oplegnathus fasciatus* male**	***Oplegnathus fasciatus* female**
SINE (%)	0.42	0.63	0.89	0.53	1.01	1.33	0.25	0.12
LINE (%)	2.76	2.76	5.1	2.72	12.39	11.31	7.08	7.34
LTR (%)	2.85	1.79	1.41	0.9	10.99	5.20	4.11	4.00
DNA (%)	4.74	5.24	10.06	7.25	16.63	20.06	10.55	11.95
Tandem repeats (%)	2.03	2.7	0.92	2.81	1.06	/	1.03	1.01
Total (%)	16.12	18.63	28.59	21.88	39.75	38.59	23.16	23.62

Table S8. Repeat content in female *Ch8*, *Ch10* and male *Ch9* of *O. fasciatus*, Related to Figure S5 and Table 3.

Repeat types	**Female *Ch8***	**Female *Ch10***	**Male *Ch9***
SINE (%)	0.06	0.1	0.17
LINE (%)	7.24	5.98	7.10
LTR (%)	3.52	3.75	5.02
DNA (%)	13.31	11.06	10.23
Tandem repeats (%)	0.81	0.91	0.87
Total (%)	26.07	22.70	23.79

Table S9. Transcriptome data from RNA-seq for male *O. fasciatus*, Related to Table 4.

Sample	Before filter			After filter			Gene No.	Read N50	Max length	Average length
	Before filter data (bp)	Q20 (%)	Q30 (%)	After filter data (bp)	Q20 (%)	Q30 (%)	62,467	2,450 bp	59,651 bp	1,214 bp
CK-1	4 193 837 760	96.13	91.49	3,946,007,277	98.13	94.56				
CK-2	4 542 887 548	96.23	91.66	4,287,840,962	98.16	91.61				
CK-3	3 707 145 734	97.34	93.32	3,557,038,640	98.45	95.12				
VC-1	3 855 448 572	97.42	93.49	3,703,645,388	98.49	95.23				
VC-2	4 565 074 582	97.40	93.44	4,386,344,462	98.47	95.19				
VC-3	4 180 130 282	97.34	93.30	4,012,959,725	98.45	95.10				
TP-1	3 379 514 994	97.35	93.32	3,242,985,938	98.45	95.13				
TP-2	3 281 341 740	97.43	93.47	3,157,433,918	98.47	95.16				
TP-3	3 647 614 890	97.45	93.55	3,509,897,398	98.50	95.25				
NC-1	3 398 536 162	97.44	93.52	3,268,777,185	98.49	95.22				
NC-2	3 404 172 992	97.44	93.53	3,276,779,782	98.48	95.24				
NC-3	3 488 720 308	97.51	93.66	3,359,820,359	98.52	95.31				

*The data was cited from the reference Xiao et al., 2019.

Table S10. Gene annotation of male *O. fasciatus* genome, Related to Figure 1, Figure 3 and Table 4.

Gene set		Number	Average gene length (bp)	Average CDS length (bp)	Average exon per gene	Average exon length (bp)	Average intron length (bp)
De novo	AUGUSTUS	29,784	13,418.44	1,453.16	8.34	174.34	1,631.18
	Genscan	35,112	16,257.97	1,524.37	8.61	177.15	1,937.33
Homolog	*Larimichthys crocea*	46,228	9,281.13	1,115.50	5.93	188.27	1,657.97
	Lates calcarifer	47,999	9,284.06	1,128.68	5.94	190	1,650.76
	Gasterosteus aculeatus	38,627	8,821.88	1,063.55	6.14	173.25	1,509.74
	Paralichthys olivaceus	40,557	8,970.29	1,114.68	6.08	183.25	1,545.55
	Cynoglossus semilaevis	40,155	9,646.94	1,132.68	6.16	183.83	1,649.56
	Gadus morhua	12,282	8,739.86	966.93	6.03	160.24	1,543.95
RNAseq		20,297	15,195.19	1,242.78	8.74	340.38	1,578.61
BUSCO		4,781	13,202.83	1,956.20	12.3	159.09	995.60
MAKER		24,357	17,192.56	1,740.06	10.31	251.18	1,569.42
HICESAP		24,835	15,819.40	1,707.02	10.01	220.05	1,511.67

Table S11. The annotation of non-coding RNAs of male *O. fasciatus* genome, Related to Table 2.

Type		Copy	Average length (bp)	Total length (bp)	% of genome
miRNA		593	85.66	50,797	0.0064
tRNA		921	75.28	69,329	0.0087
rRNA	rRNA	134	193.52	25,932	0.0033
	18S	7	1,668.86	11,682	0.0015
	28S	0	0.00	0	0.0000
	5.8S	5	156.00	780	0.0001
	5S	122	110.41	13,470	0.0017
	8S	0	0.00	0	0.0000
snRNA	snRNA	442	135.07	59,701	0.0075
	CD-box	127	109.98	13,967	0.0018
	HACA-box	75	144.15	10,811	0.0014
	Splicing	231	143.28	33,098	0.0042
	scaRNA	9	202.78	1,825	0.0002

Table S12. Homology comparisons of chromosomal sequences and genes between female $X_1X_1X_2X_2$ and male X_1X_2Y corresponding to the female *Ch8*/*Ch10* and the male *Ch9* of *O. fasciatus*, Related to Figure 3 and Table S4.

	Female *Ch8* vs male *Ch9*	Female *Ch10* vs male *Ch9*	Male *Ch9* vs female *Ch8*/*Ch10*
*Total length of homology sequences	31,327,076 bp	31,843,995 bp	63,130,076 bp
**Percentages of whole chromosome length for homology sequences	83.36%	90.14%	66.99%
Total numbers of genes	1194	1139	3064
Numbers of homologous genes	1041	968	2809
Coverage ratios of homologous genes	87.19%	84.99%	91.68%

*Aligned by using MUMmer with nucmer -num -l 100 -c 1000 -D5; delta-filter -i 95 -o 95 -1.

**Aligned by ncbi-blast-2.2.29+ with parameter 1e-5 using the gene CDS sequences.

Table S13. Statistics of the rest chromosomal sequences (33.0%) of the male *Ch9* compared to the whole female genome of *O. fasciatus* by using MUMmer with parameter setting of mum -l 100 -c 100 -D 5, Related to Figure 3 and Figure S5.

	The rest chromosomal sequences of the male Ch9 with length more than 10 kb	Alignment to the whole female genome	Unaligned to the whole female genome	Only aligned to the female *Ch8*	Only aligned to the female *Ch10*	Both aligned to the female *Ch8* and *Ch10*	Others
Total length	29,925,193 bp	22,703,944 bp	7,221,249 bp	15,763,128 bp	4,333,338 bp	343,922 bp	2,951,400 bp
Ratios		75.87%	24.13%	52.68%	14.48%	1.15%	9.86%

Table S14. Representatives of 172 male-specific genes with location and annotation details of *O. fasciatus*, Related to Figure 3.

Male_Chr9	**Gene_start**	**Gene_end**	**Gene_ID**	**NR_def**	**GO_ID**	**GO_term**	**KO_ID**	**KO_gene**	**KEGG Pathway**
Chr9	392143	395375	Ofa000011	Uncharacterized protein LOC109083330 [Cyprinus carpio]	GO:0005654; GO:0007010; GO:0000981; GO:0022604; GO:0007275; GO:0008270; GO:0005737; GO:0003677	Nucleoplasm; cytoskeleton organization; RNA polymerase II transcription factor activity, sequence-specific DNA binding; regulation of cell morphogenesis; multicellular organism development; zinc ion binding; cytoplasm; DNA binding	-	-	-
Chr9	**5305798**	**5328719**	**Ofa000102**	[Larimichthys crocea]	GO:0031110	Regulation of microtubule polymerization or depolymerization	-	-	-
Chr9	**10475126**	**10483190**	**Ofa000279**	Synaptonemal complex protein 1 [Oreochromis niloticus] > XP_013132081.1 PREDICTED: synaptonemal complex protein 1 [Oreochromis niloticus]; XP_005458454.1 PREDICTED: synaptonemal complex protein 1 [Oreochromis niloticus] > XP_005458453.1 PREDICTED: synaptonemal complex protein 1 [Oreochromis niloticus] >	-	-	K19533	SYCP1	-
Chr9	16925807	16926699	Ofa000496	Caveolin-3-like [Scleropages formosus]	GO:0016020; GO:0000139; GO:0016021; GO:0032947; GO:0005901;	Membrane; Golgi membrane; integral component of membrane; protein complex scaffold activity; caveola; regulation of signaling; muscle cell cellular homeostasis;	K12959	CAV3	Focal adhesion;Endocytosis

					GO:0023051; GO:0046716; GO:0070836; GO:0005886; GO:0044325; GO:0005794	caveola assembly; plasma membrane; ion channel binding; Golgi apparatus			
Chr9	**19585888**	**19589330**	**Ofa000610**	Microfibrillar-associated protein 2 isoform X1 [Larimichthys crocea] > XP_019128312.1 PREDICTED: microfibrillar-associated protein 2-like isoform X1 [Larimichthys crocea]	-	-	-	-	-
Chr9	20468886	20471223	Ofa000667	Splicing factor 3 [Larimichthys crocea]; serine/arginine-rich splicing factor 3 isoform X1 [Larimichthys crocea]	GO:0000166; GO:0003676	Nucleotide binding; nucleic acid binding	K12892	SFRS3	Spliceosome
Chr9	**46210055**	**46211646**	**Ofa001651**	Protein P [Larimichthys crocea]	GO:0034080; GO:0000775	CENP-A containing nucleosome assembly; chromosome, centromeric region	K11508	CENPP	-
Chr9	**23563653**	**23568436**	**Ofa000846**	Nuclear receptor subfamily 4 group A member 1-like, partial [Larimichthys crocea]	GO:0043565; GO:0003707; GO:0046872; GO:0008270; GO:0003677; GO:0005634; GO:0006355; GO:0043401; GO:0004879; GO:0003700; GO:0006351	Sequence-specific DNA binding; steroid hormone receptor activity; metal ion binding; zinc ion binding; DNA binding; nucleus; regulation of transcription, DNA-templated; steroid hormone mediated signaling pathway; RNA polymerase II transcription factor activity, ligand-activated sequence-specific DNA binding; transcription factor activity, sequence-specific DNA binding; transcription, DNA-templated	K04465	NR4A1,HMR	MAPK signaling pathway; PI3K-Akt signaling pathway; Aldosterone synthesis and secretion
Chr9	67479363	67485472	Ofa002284	Protein regulator of cytokinesis 1-like isoform X1 [Lates calcarifer]	GO:0008017; GO:0001578; GO:0000910; GO:0005856;	Microtubule binding; microtubule bundle formation; cytokinesis; cytoskeleton; microtubule cytoskeleton organization	K16732	PRC1	-

Chr9	**85600993**	**85602200**	**Ofa002902**	Transmission fidelity protein 8 [Anoplopoma fimbria]	GO:0000226 GO:0031390; GO:0007064	Ctf18 RFC-like complex; mitotic sister chromatid cohesion	K11270	CTF8	-

Note: The details of 172 male-specific genes with location and annotation of *O. fasciatus* in the suppinforation file.

Table S15. Coverage ratios of homologous genes from the synteny blocks in chromosomes of Barred knifejaw and Medaka (female Barred knifejaw vs male Barred knifejaw and Medaka vs male Barred knifejaw), Related to Figure 4, Figure S6.

Chromosome ID of female Barred knifejaw	**Chromosome ID of male Barred knifejaw**	**Chromosome ID of Medaka**	**Coverage ratio of female Barred knifejaw** (**female** *O. fasciatus* vs male *O. fasciatus*)	**Coverage ratio of male Barred knifejaw** (male *O. fasciatus* vs *O. latipes*)	**Coverage ratio of Medaka** (*O. latipes* vs male *O. fasciatus*)
fechr_1	machr_1	olch2	81.02%	44.07%	43.30%
fechr_2	machr_2	olch4/olch17	86.97%	56.57%/0.70%	50.99%/0.59%
fechr_3	machr_3	olch16	87.52%	58.19%	61.14%
fechr_4	machr_4	olch7	86.43%	58.52%	63.60%
fechr_5	machr_5	olch3	86.16%	53.82%	57.96%
fechr_6	machr_6	olch1/olch8	79.35%	46.44%/0.90%	52.25%/0.97%
fechr_7	machr_7	olch13/olch14	81.97%	52.34%/0.78%	53.07%/0.82%
fechr_9	machr_8	olch21	84.13%	48.32%	47.38%
fechr_8 fechr_10	machr_9	olch5/olch6/olch23	82.63%/82.18%	23.79%/19.06%/0.16%	51.67%/55.77%/0.89%
fechr_11	machr_10	olch24	76.53%	45.31%	44.87%
fechr_12	machr_11	olch15/olch19	85.27%	51.39%/2.41%	50.77%/2.62%
fechr_13	machr_12	olch10	84.79%	55.27%	61.34%
fechr_14	machr_13	olch18	63.49%	46.92%	54.35%
fechr_15	machr_14	olch22	85.82%	50.87%	49.47%
fechr_16	machr_15	olch20	83.86%	58.69%	61.00%
fechr_17	machr_16	olch12	87.07%	54.93%	54.50%
fechr_18	machr_17	olch19/olch15	84.49%	53.84%/1.72%	61.47%/1.79%
fechr_19	machr_18	olch9	84.86%	60.54%	57.34%
fechr_20	machr_19	olch23	82.26%	55.26%	62.97%

fechr_21	machr_20	olch11/olch16	83.44%	50.40%/1.36%	48.63%/1.12%
fechr_22	machr_21	olch8/olch19	84.89%	62.40%/0.62%	62.49%/0.92%
fechr_23	machr_22	olch17	84.42%	63.70%	58.26%
fechr_24	machr_23	olch14/olch13	78.13%	53.08%/1.11%	53.64%/1.09%

Note: The details of homology locations between Barred knifejaw and Medaka in the suppinforation file.

Transparent Methods

METHOD DETAILS

Sample collection and sequencing

A male *O. fasciatus* captured from the location (35.49N, 119.69E) of Qingdao city (Yellow Sea), Shandong province was used for genome sequencing and assembly. High-quality genomic DNA was extracted from the muscle and blood samples of the same male *O. fasciatus* individual using the PacBio sequel platform (Pacific Biosciences of California, Menlo Park, CA, USA) and the Illumina HiSeq X Ten platform (Illumina Inc., San Diego, CA, USA), respectively. Two genomic DNA libraries (20 kb) were constructed using the manufacturer's protocol provided by the Pacific Biosciences. Sequencing was conducted using Sequel Binding Kit 2.0, Sequel Sequencing Kit 2.1 and Sequel SMRT Cell 1M v2 on the PacBio sequel platform. Five SMRT Cells were used for the male genome sequencing and SMRT LINK 5.0 was used to filter the raw data from the zero-mode waveguide.

To obtain a chromosome-level genome assembly for male *O. fasciatus*, a Hi-C library was constructed for sequencing. The whole blood from the same male *O. fasciatus* individual was extracted for Hi-C library construction. The blood cells were cross-linked using formaldehyde and then lysed. A restriction enzyme (MboI) was used to digest the cross-linked DNA, and then, the sticky ends were filled and marked with biotin. Then, the biotin-labelled chromosomes in proximity were ligated to create chimeric junctions representing their physical interactions in the chromosome system. Finally, the cross-linked DNA was unlinked using a protease, and the chimeric junctions of the genome were sheared to a size of 300-500 bp (Belaghzal et al., 2017). A PE library with an approximately 300 bp insert size was constructed according to the Illumina library preparation protocol (Illumina Inc., San Diego, CA, USA). The sequencing of the Hi-C library was conducted using the Illumina HiSeq X Ten platform (Illumina) with a read length of 150 bp for each end.

High-quality RNA was also extracted from the eggs of *O. fasciatus* for genome annotation, and sequencing was performed using the Illumina HiSeq X Ten in 150PE

mode (Xiao et al. 2019).

Genome assembly of the male *O. fasciatus* genome

The genome size of female *O. fasciatus* was estimated using a 17-mer frequency distribution analysis (Marcais & Kingsford 2011; Xiao et al. 2019). The genome size of female *O. fasciatus* was calculated to be 777.5 Mb with a heterozygous ratio of 0.29% and a repeat percentage of 38.46% (Xiao et al. 2019). According to the genome survey of female *O. fasciatus* combined with the subreads obtained using the PacBio Sequel platform, the Canu v1.4 with the Corrected-Error-Rate parameter set to 0.040 was first used to complete the *de novo* assembly of the male *O. fasciatus* genome (Koren et al. 2017). And then, the Redundans v0.13c was used to remove sequence redundancy with the minCoverage parameter of 15 and the Arrow tool in SMRT Link 5.0 software was used to polish genome sequence using long-read sequencing data (Pryszcz & Gabaldón, 2016; Chin et al., 2013). Finally, the Pilon software was applied to polish the assembly genome using the Illumina NGS short reads mentioned in the genome survey of female *O. fasciatus* (Walker et al., 2014).

The high-quality Hi-C data was further used to assist the genome assembly of the male *O. fasciatus* to a chromosome level. The reads from the Hi-C library sequencing were first mapped to the polished genome using BWA software with default parameters (Li & Durbin, 2009). To avoid the influence of long reads, reads apart from each restriction sites more than 500bp were filtered out using BWA and Lachesis software (Burton et al., 2013). And then the Lachesis software with tuned parameters was used to cluster, order and orientate the contigs using their contact frequencies. Finally, the Juicer software with JucieBox was combined to construct a physical map of chromosome interactions and complete the visual correction with the interaction map (Durand et al., 2016). LOWESS method (alpha = 0.5%, ignore zeros, IQR filter) was explored to model the overall chromatin interaction decay with distance (Sanyal et al., 2012). Cumulative distribution of subtraction Hi-C using Z-scores values for interactions between 400 kb and 40 kb bins were carried out from the whole genome and chromosome levels.

Genome quality evaluation for the male *O. fasciatus*

First, the Minimap2 software using the CLR (continuous long reads) data was employed to evaluate the completeness and homogeneity of the assembled genome with default settings (Li, 2018). Then, the completeness of the assembled genome was evaluated using BUSCO v3 software with the actinopterygii_odb9 database (Simão et al., 2015). Finally, the BWA software (BWA, RRID: SCR_010910) with the default settings was applied to align the NGS-based short reads from the whole-genome sequencing data to the reference genome and evaluated the accuracy of the assembled genome based on the called SNP loci using GATK (Li & Durbin, 2009; Mckenna et al., 2010).

Repetitive element annotation and protein-coding gene prediction

We used The Tandem Repeat Finder was used to detect repetitive elements in the male *O. fasciatus* genome (Benson, 1999). A *de novo* repeat library of the male *O. fasciatus* genome was constructed using Repeat Modeler (version 1.04) and LTR_FINDER with default parameters. The known and novel transposable elements (TEs) were identified using Repeat Masker (version 3.2.9) from the Repbase TE database (version 14.04) and the *de novo* repeat library (Tarailo-Graovac & Chen, 2009). The TE-relevant proteins in the assembled genome were also identified using Repeat Protein Mask software (version 3.2.2) (Tarailo-Graovac & Chen, 2009).

The prediction of protein-coding genes in the assembled genome of male *O. fasciatus* was conducted using three approaches: homology, *de novo* and transcriptome sequencing. Protein sequences of *Lates calcarifer*, *Larimichthys crocea*, *Gasterosteus aculeatus*, *Gadus morhua*, *Paralichthys olivaceus* and *Cynoglossus semilaevis* were obtained from Ensembl and used for the homology annotation (Flicek et al., 2014). Then, the TBLASTN software with an e-value threshold of 1E-5 was used to align protein sequences to the assembled genome of male *O. fasciatus*. Finally, the Genewise2.2.0 software was employed to predict potential gene structures based on all alignments. Augustus (version 2.5.5) and Genscan (version 1.0) software were used for *de novo* prediction of protein-coding genes (Burge & Karlin, 1997; Stanke et al., 2004). Augustus was trained with the gene set from the homology annotation. Simultaneously, the TopHat 1.2 software was used to map the transcriptome

sequencing reads to the assembled genome (Trapnell et al., 2009). The Cufflinks software was then applied to predicate the potential gene structures based on the sorted and integrated alignments using TopHat software. Finally, the MAKER software was employed to obtain a comprehensive and non-redundant gene set by merging the annotation results of the abovementioned annotation pipelines (Campbell et al., 2014).

Functional annotation of predicted protein-coding genes

To complete the functional annotation of predicted genes in the male *O. fasciatus* genome, all protein sequences were aligned against the Swiss-Prot, the non-redundant nucleotide (NT) and non-redundant protein (NR) database using local BLASTX and BLASTN programs with an e-value threshold of 1E-5 (Lobo, 2008; Altschul et al., 2012). The Blast2GO software was then used to perform the annotation of the Gene Ontology (GO) annotation (Harris et al., 2004; Conesa et al., 2005). The best hit for each protein genes coupled with a biological pathway was also identified using the Kyoto Encyclopaedia of Genes and Genomes (KEGG) pathway database (Ogata et al., 2000). In addition, tRNAscan-SE and the Rfam database were also used to annotate the non-coding RNAs (microRNAs, transfer RNAs, ribosomal RNAs, and small nuclear RNAs) with default settings (Lowe & Eddy, 1997; Griffiths-jones et al., 2003).

Chromosome comparison with synteny analysis

The synteny relationships between the male and female *O. fasciatus* genomes were determined using the program MUMmer 3.23 (http://mummer.sourceforge.net/) with the default settings (Kurtz et al., 2004). The alignment results were filtered for more than 85% identity and visualized using the mummer plot (Delcher et al., 2003). Synteny analyses were also performed among the male/female *O. fasciatus* genomes and *L. crocea* genomes to detect syntenic blocks. According to the annotated protein-coding genes of male and female *O. fasciatus*, precise gene pairs from the male and female *O. fasciatus* chromosomes was identified based on their synteny and homological searching with BLASTP software with identity ≥ 95% and e-value ≤ 1E-5. The homology comparision of chromosomal sequences between the female

$X_1X_1X_2X_2$ and the male X_1X_2Y were also analyzed using nucmer software with parameter settings (mum -l 100 -c 1000/100 -D 5). The BLASTN software with an e-value threshold of 1E-5 was further used to compare genes between male *Ch9* and female genome based on the CDS. The mapping results mentioned above were merged into a circos plot using Circos v0.69 software (Krzywinski et al., 2009). The chromosomal structures between *Oryzias latipes* genome (Japanese medaka with the normal XY system, ASM31367v1) and *O. fasciatus* genome (Barred knifejaw with the X_1X_2Y system) were identified using JCVI v0.7.5 (https://github.com/tanghaibao/jcvi) with minspan=30 –simple (Tang et al., 2017). The order of the corresponding chromosomes for the male/female *O. fasciatus* and *L. crocea* followed the standard of male *O. fasciatus* as *Chr1* to *Chr23*. The chromosomes named for the male/female *O. fasciatus* were designated machr and fechr, respectively.

Gene family identification for evolutionary analysis

To identify the gene families for phylogenetic tree construction, we used the genome of male *O. fasciatus* for comparisons with those of other marine species, including *Salmo salar*, *Larimichthys crocea*, *Gadus morhua*, *Paralichthys olivaceu*, *Cynoglossus semilaevis*, *Notothenia coriiceps*, *Boleophthalmus pectinirostris*, *Branchiostoma floridae*, *Gasterosteus aculeatus*, *Callorhinchus milii*, *Danio rerio* and *Oryzias latipes*. To obtain high-confidence results, the protein sequences of the longest transcript of each gene for the abovementioned species were selected. The BLASTP program was used to search for similarities between the protein sequences in an all-to-all manner with an e-value threshold of 1E-5 (Altschul et al., 2012). Finally, the Hcluster_sg software (https://github.com/dougl asgsc ofiel d/hcluster) was employed to obtain the clustering of gene families based on H-scores calculated from the bit-score.

Phylogenetic analysis and divergence time estimation

The phylogenetic relationships between male *O. fasciatus* and the abovementioned species were constructed using orthologues. We used OrthoMCL V2.0.9 software to generate orthologous groups with a coefficient setting of 1.5 (Li et al., 2003). The

ClustalW program was applied to extract and align the protein sequences of single-copy genes from the orthogroups with a length filter (retention of proteins wtih length≥100 aa) (Thompson et al., 2002). Then, the MUSCLE software was used to conduct multiple sequence alignments for each of single-copy genes from male *O. fasciatus* and other marine species (Edgar, 2004). All of the coding sequence alignments were concatenated to form a super-alignment data set for each species. RAxML software was implemented to estimate phylogenetic relationships among species using the maximum-likelihood method (Stamatakis, 2014). According to the eight calibration times obtained from the TimeTree database (http://www.timetree.org/), MCMCtree as implemented in the PAML package was employed to predict the divergence times among species (Yang, 2007).

Supplemental References

Altschul, S.F., Gish, W., Miller, W., Myers, E.W., and Liponan, D.J. (2012). Basic local alignment search tool (BLAST). J. Mol. Biol. *215*, 403-410.

Belaghzal, H., Dekker, J., and Gibcus, J.H. (2017). HI-C 2.0: An optimized Hi-C procedure for high-resolution genome-wide mapping of chromosome conformation. Methods *123*, 56-65.

Benson, G. (1999). Tandem repeats finder: A program to analyze DNA sequences. Nucleic Acids Res. *27*, 573.

Burge, C., and Karlin, S. (1997). Prediction of complete gene structures in human genomic DNA. J. Mol. Biol. *268*, 78-94.

Burton, J.N., Adey, A., Patwardhan, R.P., Qiu, R., Kitzman, J.O., and Shendure, J. (2013). Chromosome-scale scaffolding of de novo genome assemblies based on chromatin interactions. Nat. Biotechnol. *31*, 1119-1125.

Campbell, M.S., Holt, C., Moore, B., and Yandell, M. (2014). Genome Annotation and Curation Using MAKER and MAKER-P. Curr. Protoc. Bioinformatics *48*, 4.11.11.

Chin, C.S., Alexander, D.H., Marks, P., Klammer, A.A., Drake, J., Heiner, C., Clum, A., Copeland, A., Huddleston, J., Eichler, E.E., Turner, S.W., and Korlach, J. (2013). Nonhybrid, finished microbial genome assemblies from long-read SMRT sequencing data. Nat. Methods *10*, 563.

Cioffi, M.B., and Bertollo, L.A.C. (2012). Chromosomal distribution and evolution of repetitive DNAs in fish. Repetit. DNA *7*, 197-221.

Conesa, A., Götz, S., García-Gómez, J.M., Terol, J., Talón, M., and Robles, M. (2005). Blast2GO: universal tool for annotation, visualization and analysis in functional genomics research. Bioinformatics *21*, 3674.

Delcher, A.L., Salzberg, S.L., and Phillippy, A.M. (2003). Using MUMmer to identify similar regions in large sequence set. Current Protocol in Bioinformatics Chapter 10: Unit 10.3.

Durand, N.C., Shamim, M.S., Machol, I., Rao S.S.P., Huntley, M.H., Lander, E.S., and Aiden E.L. (2016). Juicer provides a one-click system for analyzing loop-resolution Hi-C experiments. Cell Syst. *3*, 95-98.

Edgar, R.C. (2004). MUSCLE: multiple sequence alignment with high accuracy and high throughput. Nucleic Acids Res. *32*, 1792-1797.

Flicek, P., Amode, M.R., Barrell, D., Beal, K., Billis, K., Brent, S., Carvalho-Silva, D., Clapham, P., Coastes, G., Fitzgerald, S., et al. (2014). Ensembl 2014. Nucleic Acids Res. *42* (Database issue), D749–D755.

Gong, G.R., Dan, C., Xiao, S.J., Guo, W.J., Huang, P.P., Xiong, Y., Wu J.J., He, Y., Zhang, J.C., Li, X.H., et al., (2018). Chromosomal-level assembly of yellow catfish genome using third-generation DNA sequencing and Hi-C analysis. GigaScience *7*, giy120.

Griffithsjones, S., Bateman, A., Marshall, M., Khanna, A., and Eddy, S.R. (2003). Rfam: An RNA family database. Nucleic Acids Res. *31*, 439-441.

Harris, M.A., Clark, J., Irenland, A, Lomax, J., Ashiburner, M., Foulger, R., Eilbeck, K., Lewis, S., Marshall, B, Mungall, C., et al. (2004). The Gene Ontology (GO) database and informatics resource. Nucleic Acids Res. *32*, 258D-261.

Koren, S., Walenz, B.P., Berlin, K., Miller, J.R. Bergman, N.H., and Phillippy, A.M. (2017). Canu: scalable and accurate long-read assembly via adaptive *k*-mer weighting and repeat separation. Geneome Res. *27*, 722-736.

Krzywinski, M., Schein1, J., Birol1, İ., Connors, J., Gascoyne, R., Horsman, D., Jones, S.J., and Marra1, M.A. (2009). Circos: An information aesthetic for comparative genomics. Geneome Res. *19*, 1639-1645.

Kurtz, S., Phillippy, A., Delcher, A., Smoot, M., Shumway, M., Antonescu, C., and Salzberg, S.L. (2004). Versatile and open software for comparing large genomes. Genome Biol. *5*, R12.

Li, H. (2018). Minimap2: pairwise alignment for nucleotide sequences. Bioinformatics *34*,

3094-3100.

Li, H., and Durbin. R. (2009). Fast and accurate short read alignment with Burrows–Wheeler transform. Bioinformatics *25*, 1754-1760.

Li, L., Stoeckert, C.J., and Roos, D.S. (2003). OrthoMCL: Identification of Ortholog Groups for Eukaryotic Genomes. Genome Res. *13*, 2178-2189.

Lobo, I. (2008). Basic local alignment search tool (BLAST). Nature Educat. 1.

Lowe, T.M., and Eddy, S.R. (1997). tRNAscan‐SE: A program for improved detection of transfer RNA genes in genomic sequence. Nucleic Acids Res. *25*, 955-964.

Marçais, G., and Kingsford, C. (2011). A fast, lock-free approach for efficient parallel counting of occurrences of k-mers. Bioinformatics *27*, 764.

McKenna, A., Hanna, M., Banks, E., Sivachenko, A., Cibulskis, K., Kernytsky, A., Garimell, K., Altshuler, D., Gabriel, S., Daly, M., et al. (2010). The Genome Analysis Toolkit: A MapReduce framework for analyzing next-generation DNA sequencing data. Genome Res. *20*, 1297-1303.

Ogata, H., Goto, S., Sato, K., Fujibuchi, W., Bono, H., and Kanehisa, M. (2000). KEGG: kyoto encyclopedia of genes and genomes. Nucleic Acids Res. *27*, 29-34.

Pryszcz, L.P., and Gabaldón, T. (2016). Redundans: an assembly pipeline for highly heterozygous genomes. Nucleic Acids Res. *44*, e113-e113.

Simão, F.A., Waterhouse, R.M., Ioannidis, P., Kriventseva, E.V., and Zdobnov E.M. (2015). BUSCO: assessing genome assembly and annotation completeness with single-copy orthologs. Bioinformatics *31*, 3210-3212.

Stamatakis, A. (2014). RAxML version 8: a tool for phylogenetic analysis and post-analysis of large phylogenies. Bioinformatics *30*, 1312-1313.

Stanke, M., Steinkamp, R., Waack, S., and Morgenstern, B. (2004). AUGUSTUS: a web server for gene finding in eukaryotes. Nucleic Acids Res. *32*, W309-W312.

Sanyal, A., Lajoie, B.R., Jain, G. and Dekker, J. (2012). The long-range interaction landscape of gene promoters. Nature *489*, 109-113.

Tarailo-Graovac, M., and Chen, N. (2009). Using RepeatMasker to identify repetitive elements in genomic sequences. Current Protocols in Bioinformatics, Chapter 4, Unit 4.10.

Thompson, J.D., Gibson, T.J., and Higgins, D.G. (2002). Multiple sequence alignment using

ClustalW and ClustalX. Current Protocols in Bioinformatics, 4.10.1-4.10.14 1-14.

Trapnell, C, Pachter, L., and Salzberg, S.L. (2009). TopHat: discovering splice junctions with RNA-Seq. Bioinformatics *25*, 1105-1111.

Tang, H.B., Krishnakumar, V., Li, J.P., MicchelMoser, Maria, and Cheol Yim W. (2017). Jcvi v0.7.5: JCVI utility libraries. Zenodo. doi:10.5281/zenodo.31631.

Walker, B., Abeel, T., Shea, T., Priest, M., Abouelliel, A., Sakthikumar, S., Cuomo, C.A., Zeng, Q.D., Wortman, J., Yong, S.K., et al. (2014). Pilon: An integrated tool for comprehensive microbial variant detection and genome assembly improvement. PLOS one *9*, e112963.

Xiao, Y.S., Xiao, Z.Z., Ma, D.Y., Liu, J. and Li, J. (2019). Genome sequence of the barred knifejaw Oplegnathus fasciatus (Temminck & Schlegel, 1884): the first chromosome-level draft genome in the family Oplegnathidae. GigaScience *8*, giz013.

Yang, Z.H. (2007). PAML 4: Phylogenetic Analysis by Maximum Likelihood. Mol. Biol. Evol. *24*, 1586-1591.